

Linearized Lorentz-Violating Gravity and Discriminant Locus in the Moduli Space of Mass Terms

Andrei Mironov*, Sergey Mironov†, Alexei Morozov‡ and Andrey Morozov§

October 24, 2018

Abstract

We analyze the pattern of normal modes in linearized Lorentz-violating massive gravity over the 5-dimensional moduli space of mass terms. Ghost-free theories arise at bifurcation points when the ghosts get out of the spectrum of propagating particles due to vanishing of the coefficient in front of ω^2 in the propagator. Similarly, the van Dam-Veltman-Zakharov (DVZ) discontinuities in the Newton law arise at another type of bifurcations, when the coefficient vanishes in front of \vec{k}^2 . When the Lorentz invariance is broken, these two kinds of bifurcations get independent and one can easily find a ghost-free model without the DVZ discontinuity in the moduli space, at least, in the quadratic (linearized) approximation.

1. Introduction. The theory of massive gravity [1, 2] attracts a new attention these days [3, 4] because of the growing belief in acceleration of Universe expansion (the "dark energy" phenomenon) [5].¹ However, the violation of general covariance in massive gravity is long known to produce a number of non-trivial effects like occurrence of ghosts and the lack of perturbative regime at small distances [8], moreover, the van Dam-Veltman-Zakharov (DVZ) discontinuities [9, 10] and the Boulware-Deser instabilities [11] arise whenever one tries to eliminate the ghosts. In fact, these problems can probably be avoided, if one sacrifices the Lorentz invariance [12, 3], what allows to extend the number of possible mass terms and go around the most unpleasant singularities in the moduli space. This was demonstrated at the level of the linearized gravity with quadratic action²

$$K_{\mu\nu,\alpha\beta}h^{\mu\nu}h^{\alpha\beta} = \left\{ \frac{1}{2} \left(k_\mu k_\alpha \eta_{\beta\nu} + k_\mu k_\beta \eta_{\alpha\nu} + k_\nu k_\alpha \eta_{\beta\mu} + k_\nu k_\beta \eta_{\alpha\mu} \right) - \left(k_\mu k_\nu \eta_{\alpha\beta} + k_\alpha k_\beta \eta_{\mu\nu} \right) - \frac{1}{2} k^2 \left(\eta_{\mu\alpha} \eta_{\nu\beta} + \eta_{\nu\alpha} \eta_{\mu\beta} \right) + k^2 \eta_{\mu\nu} \eta_{\alpha\beta} \right\} h^{\mu\nu} h^{\alpha\beta} + m_0^2 h_{00}^2 + 2m_1^2 h_{0i}^2 - m_2^2 h_{ij}^2 + m_3^2 h_{ii}^2 - 2m_4^2 h_{00} h_{ii}, \quad (1)$$

where the first line is nothing but quadratic approximation to the Einstein-Hilbert action, while the second line contains five different mass terms,³ which violate both gauge (general coordinate) and Lorentz $SO(d-1, 1)$ invariance, but preserve space rotation symmetry $SO(d-1)$. In our notation, $h_{ii}^2 = \left(\sum_{i=1}^{d-1} h_{ii} \right)^2$, while $h_{ij}^2 = \sum_{i,j=1}^{d-1} h_{ij}^2$. The theory also has the P and T reflection symmetries, so that all scalar physical quantities

* *Lebedev Physics Institute and ITEP, Moscow, Russia*; mironov@itep.ru; mironov@lpi.ru

† *Moscow State University and ITEP, Moscow, Russia*; badzilla@rambler.ru

‡ *ITEP, Moscow, Russia*; morozov@itep.ru

§ *Moscow State University and ITEP, Moscow, Russia*; Andrey.Morozov@itep.ru

¹ As we understand, the argument is as follows. There is an experimental evidence that cosmological constant is actually non-vanishing. From the point of view of flat geometry, the cosmological constant makes graviton massive (in fact it also provides it with a source term, linear in h , therefore a more accurate analysis, including the change of expansion background, is actually required), then, Lorentz-invariant massive gravity looks ill, but this can be cured by switching on especially adjusted Lorenz-violating terms, perhaps as small as the cosmological constant, what makes their effect small and consistent with existing observations. Alternatively one could say that non-vanishing negative cosmological constant implies that flat background geometry is substituted with AdS one, and all analysis should be made differently from this new perspective [6]. In fact motivations for the study of infrared-modified gravity are not exhausted by the dark-energy problem, for some other examples see [3] and [7].

² Throughout the paper, our convention for the metric signature is $(-, +, \dots, +)$.

³ Of course, one can violate Lorentz invariance not only in the sector of masses, but also in kinetic term and add higher derivatives in space directions, which do not produce new ghosts. For profound example of this kind see [13]. The methods of the present paper are straightforwardly applicable to these non-minimal deformations, but on this road the moduli space \mathcal{M} is in no way restricted and eigenvalue patterns can be made arbitrarily complicated.

depend on the squares ω^2 and \vec{k}^2 of frequencies and space momenta. **The Lorentz invariance** is restored if the five mass parameters can be expressed through only two independent quantities, A and B :

$$\begin{aligned} m_0^2 &= B - A, \\ m_1^2 &= m_2^2 = A, \\ m_3^2 &= m_4^2 = B \end{aligned} \tag{2}$$

and $\mathcal{K}_{\mu\nu,\alpha\beta}$ in (1) reduces to

$$\begin{aligned} &\frac{1}{2} \left(k_\mu k_\alpha \eta_{\beta\nu} + k_\mu k_\beta \eta_{\alpha\nu} + k_\nu k_\alpha \eta_{\beta\mu} + k_\nu k_\beta \eta_{\alpha\mu} \right) - \left(k_\mu k_\nu \eta_{\alpha\beta} + k_\alpha k_\beta \eta_{\mu\nu} \right) - \\ &-\frac{1}{2} (k^2 + A) \left(\eta_{\mu\alpha} \eta_{\nu\beta} + \eta_{\nu\alpha} \eta_{\mu\beta} \right) + (k^2 + B) \eta_{\mu\nu} \eta_{\alpha\beta} \end{aligned} \tag{3}$$

The ghost-free Lorentz-invariant Pauli-Fierz [1] massive gravity corresponds to the choice $A = B$: it, however, suffers from all the above-mentioned problems and thus looks unviable [3]. The Lorentz-violating theories (1) can be ghost free when either $m_0 = 0$ or $m_1 = 0$, and the second choice is the current favorite candidate for a phenomenologically acceptable version of massive gravity [3].

Lorentz violation breaks a lot of familiar properties of quantum field theory models and looks unusual in many respects. It gives rise to the whole variety of non-trivial quasi-particles which can be ghosts, superluminals and even not look like particles at all (either relativistic, or non-relativistic). In [14] we provided a systematic analysis of the theory (1) and carefully reproduced and explained the results of [3], also relating them to the obvious self-consistency of Kaluza-Klein theories, which involve massive gravitons but remain free of any kind of pathologies. Here we present this analysis in still another, concise and formal way, omitting a lot of details and physical motivations included into [14]. Note that, due to the different choice of signature, the sings of eigenvalues throughout the paper are opposite to those in [14].

2. The main quantity: the propagator $\Pi(k)$ over the moduli space. We remind briefly the standard string-theory approach to consideration of a *family* of physical theories [15], adapting it to a particular application to linearized gravity, perhaps, Lorentz-violating.

The physical content of a particular theory (model) is best expressed in terms of the partition function

$$Z(J) = \int D\phi e^{i(S(\phi) + \int J\phi)} \tag{4}$$

In quadratic approximation, when

$$S(\phi) = \int d^d k \phi(-k) K(k) \phi(k) \tag{5}$$

and

$$\int d^d x J\phi = \int d^d k J(k) \phi(k), \tag{6}$$

this $Z(J)$ is also a quadratic exponential,

$$Z(J) = \exp \left(-\frac{i}{4} \int d^d k J(-k) K^{-1}(k) J(k) \right) \tag{7}$$

made from inverse of kinetic matrix $K(k)$, i.e. the propagator. This is a finite-dimensional matrix in the space of fields $\phi(x)$: if $\phi^a(x)$ carries an index a , then $K_{ab}(k)$ carries two indices a, b . In the case of vector fields a is just the Lorentz index μ , in the case of gravitational field $a = (\mu\nu)$ is a symmetric pair of the Lorentz indices, thus taking $\frac{d(d+1)}{2}$ different values, what reduces to $\frac{(d-1)(d+2)}{2}$ in the case of the traceless field. Our main task is to investigate the quantity $\Pi(k) = J(-k) K^{-1}(k) J(k)$.

Of most interest for us in this paper are two kind of characteristics of Π .

(i) A singularity of $\Pi(k)$ defines a propagating particle and the position of the singularity defines its dispersion relation $\omega = \varepsilon(|\vec{k}|)$.

(ii) The quantity $V(|\vec{k}|) = \Pi(\omega = 0, \vec{k})$ defines an instantaneous Newton/Coulomb/Yukawa-like interaction.

The partition function Z and its quadratic approximation $\exp(-\frac{i}{4} \int \Pi)$ are of course defined over the space of theories \mathcal{M} (and are, hence, generalized τ -functions [16], ordinary and quasiclassical respectively), and we are going to study the singularities (reshufflings or bifurcations) of dispersion relations and potentials V over the moduli space \mathcal{M} . In the current problem coordinates in \mathcal{M} parameterize the kinetic matrix $K(k)$, actually, the mass terms, and, as usual in string theory, in the spirit of third-quantization, they can be considered as vacuum averages of some other fields (slow variables or moduli).

3. The notion of eigenvalues and its ambiguity. The problem of dispersion relations is basically that of the eigenvalues of $K(k)$: roughly, $\omega = \varepsilon(|\vec{k}|)$ is a condition that some eigenvalue $\lambda(k) = 0$. However, this "obvious" statement requires a more accurate formulation. The point is that K is actually a quadratic form, not an operator, what means that it can always be brought to the canonical form with only ± 1 and 0 at diagonal, thus leaving no room to quantities like $\lambda(k)$. Still, this "equally obvious" counter-statement is also partly misleading, because we are interested not in an isolated quadratic form, but in a family of those, defined over \mathcal{M} . This means that the sets of ± 1 and 0 can change as we move along \mathcal{M} , and degeneracy degree of quadratic form $K(k)$ can change. Of course, this degree (a number of 0's at diagonal) is an integer and changes abruptly – and thus is not a very nice quantity. A desire to make it smooth brings us back a concept of $\lambda(k)$. However, in order to introduce $\lambda(k)$ one needs an additional structure, for example, a metric in the space of fields.

In application to our needs one can introduce "eigenvalues" $\lambda(k)$ as follows: consider instead of $\Pi = J \frac{1}{K} J$ a more general quantity

$$\Pi(\lambda|k) = J \frac{1}{K - \lambda I} J \quad (8)$$

Then *as a function of λ* it can be represented as a sum of contributions of different poles:

$$\Pi(\lambda|k) = \sum_{a,b,c} \frac{\alpha_a^{bc} J_b J_c}{\lambda_a - \lambda} \quad (9)$$

then $\lambda_a(k)$ are exactly the "eigenvalues" that we are interested in, and our original

$$\Pi(k) = \sum_{a,b,c} \frac{\alpha_a^{bc}(k) J_b(-k) J_c(k)}{\lambda_a(k)} \quad (10)$$

The only thing that one should keep in mind is that this decomposition depends on the choice of additional matrix (metric) I , which can be chosen in different ways, in particular, its normalization can in principle depend on the point of \mathcal{M} . We shall actually assume that it does *not*, and clearly the physical properties do not depend on this choice, however, concrete expressions for $\lambda_a(k)$ do. It is important, that the dispersion relations – the zeroes of $\lambda_a(k)$ – are independent of I .

Introduction of I is also important from another point of view. To be well-defined, the Lorentzian partition function requires a distinction between the retarded and advanced correlators (Green functions), which is usually introduced by adding an infinitesimal imaginary term to the kinetic matrix K : the celebrated $i\epsilon$ in the Feynman propagator.⁴ However, in the case of kinetic *matrix* this is not just $i\epsilon$, it is rather $i\epsilon I_F$ with some particular matrix I_F . If we identify our I with I_F , then the dispersion relations are actually

$$\lambda_a(k) = i\epsilon \quad (11)$$

what implies that $\lambda_a(k)$ is, in fact, very different from $-\lambda_a(k)$, and this is related to the important concept of *ghosts*.

The most natural choices of the matrix I are probably either just the unit matrix, or "the Lorentzian unit matrix", i.e. that with -1 corresponding to the 0-components. The physically justified choice is the unit (Euclidean) matrix, while technically it is often simpler to work with the Lorentzian unit matrix, especially when dealing with theories with the Lorentz invariance unbroken. At the same time, in these two cases it is only ghost content of the non-scalar sectors which differs. Therefore, it is often safe (and technically preferable) to use the Lorentzian unit matrix. We illustrate this in the simplest warm-up example of the massive vector field theory in Appendix I, where we compare the results obtained for the two cases of Euclidean and Lorentzian eigenvalues (Euclidean and Lorentzian unit matrices). Since this paper is rather devoted to the method than to concrete physical applications, we use the Lorentzian eigenvalues here, leaving the Euclidean ones for [14], where we deal with physical issues.

⁴ The Feynman propagator implies that *particles* with the dispersion relation $\omega = +\varepsilon(|\vec{k}|)$ propagate *forward* in time, while *antiparticles* with $\omega = -\varepsilon(|\vec{k}|)$ – *backwards* in time. Since $\theta(\pm t) = \frac{1}{2\pi i} \int \frac{e^{i\omega t} d\omega}{\pm\omega - i\epsilon}$, we have for the propagator

$$\frac{1}{2\epsilon} \left(\frac{1}{\omega - \epsilon - i\epsilon} + \frac{1}{-\omega - \epsilon - i\epsilon} \right) = \frac{1}{\omega^2 - \epsilon^2 - i\epsilon}$$

For ghosts with the propagator $\frac{1}{\omega^2 - \epsilon^2 + i\epsilon}$ the situation is inverse: particles propagate backwards while antiparticles forward in time. See also Appendix II.

4. Spectrum and the phase diagram. Important information about the theory is contained in its *spectrum*: positions of the poles of $\Pi(\lambda|k)$ in the complex λ -plane. These positions define the dispersion relations $\lambda_a(\omega, \vec{k}) = 0$ between the frequency ω and the wave vector \vec{k} of elementary excitations (quasiparticles) and the way these relations depend on the point of the moduli space \mathcal{M} .

As one knows well from condensed matter physics, in generic Lorentz-violating theory dispersion relations are quite sophisticated, they are roots of polynomial equation and often do not possess any useful analytical expressions. Sometime they are better represented by pictures: the plots $\lambda_a(\omega)$ or $\lambda_a(\vec{k})$, however when the pattern is multi-dimensional one can only draw its particular $2d$ or $3d$ sections, which do not provide complete visualization. Developed algebra-geometric intuition is actually needed to analyze the spectrum – surprisingly enough, this is already the case in such a fundamental (and seemingly simple) theory as linearized gravity!

Of main interest are *qualitative* features of the spectrum and their *bifurcations*: the changes of these qualitative features when one goes from one region of the moduli space to another. The corresponding division of the moduli space into domains with qualitatively different spectra (and, perhaps, other physically relevant characteristics like structure functions $\alpha_a^{bc}(k)$) is called the *phase diagram* of the theory (or, better, of the family of theories).

5. Ghosts, tachyons, superluminals and DVZ jumps The simplest examples of qualitative features of the spectrum are the presence or absence of exotic (from the perspective of Lorentz-invariant field theory) excitations, like ghosts or superluminals.

The ghost differs from the normal particle by a sign in front of ω^2 in $\lambda_a(k)$. For example, for a scalar particle,

$$\left. \frac{\partial \lambda_a(k)}{\partial \omega^2} \right|_{\lambda_a(k)=0} \begin{array}{l} < 0 & \text{normal particle} \\ > 0 & \text{ghost} \end{array} \quad (12)$$

In order to define this sign one needs to compare it with the one in front of $i\epsilon$ in (11), see Appendix II for a more detailed discussion. Problems are actually expected when excitations with opposite signs are present: when the "ghosts" need to coexist and *interact* with the "normal" particles. The condition

$$\left. \frac{\partial \lambda_a(k)}{\partial \omega^2} \right|_{\lambda_a(k)=0} = 0 \quad (13)$$

defines the loci in the moduli space, where the ghost content of theory can change.

A similarly-looking condition

$$\left. \frac{\partial \lambda_a(\omega = 0, \vec{k})}{\partial \vec{k}^2} \right|_{\lambda_a(k)=0} = 0 \quad (14)$$

defines the loci of the **DVZ jumps**, see below. In the Lorentz invariant theory, where λ_a depends on $k^2 = -\omega^2 + \vec{k}^2$, the two conditions (12) and (14) are clearly related. Therefore, one can easily come across the DVZ jump when trying to get rid of ghosts – and this, indeed, happens in the simplest Pauli-Fierz version of linearized gravity. After the Lorentz violation, the link between (12) and (14) is relaxed.

Next, the difference between the normal particles and tachyons is as follows:

$$\begin{array}{l} \text{if } \lambda_a(\omega, \vec{k} = 0) = 0 \text{ has real solutions for the frequency } \omega, \text{ this is a normal particle,} \\ \text{if } \lambda_a(\omega = 0, \vec{k}) = 0 \text{ has real solutions for the wave vector } \vec{k}, \text{ this is a tachyon.} \end{array} \quad (15)$$

The **superluminal propagation** [17] is controlled by the group velocity

$$\vec{v}_a = \left. \frac{\partial \lambda_a(k)/\partial \vec{k}}{\partial \lambda_a(k)/\partial \omega} \right|_{\lambda_a(k)=0} \quad (16)$$

in the usual way:

$$\vec{v}_a^2 \begin{array}{l} < 1 & \text{normal particle} \\ = 1 & \text{light-like particle} \\ > 1 & \text{superluminal particle} \end{array} \quad (17)$$

In fact, it makes sense to further distinguish between different superluminals by looking at another quantity:

$$V_a^2 = \left. \frac{\partial \lambda_a(k)/\partial \vec{k}^2}{\partial \lambda_a(k)/\partial \omega^2} \right|_{\lambda_a(k)=0} \quad (18)$$

For the ordinary relativistic particle with $\lambda = -\omega^2 + \vec{k}^2 + m^2$, this $V^2 = 1$ independently of the value and even of the sign of mass m^2 . Thus, the ordinary tachyons with negative m^2 and $\vec{v}^2 > 1$ are rather "soft" superluminals. In the Lorentz violating theories things are much worse: there are "harder" superluminals with $V^2 > 1$.

Finally, the DVZ jump can occur when one of the scalars becomes infinitely heavy. Then the massless limit, when all the five moduli $m_0, \dots, m_4 \rightarrow 0$, gets ambiguous: this scalar can either remain infinitely heavy or acquire a finite mass or become massless, depending on a particular way the limit is taken. Thus, the contribution of such a scalar to the instantaneous potential is also ambiguous and depends on the way one approaches the point $m_0, \dots, m_4 = 0$: if we are interested in physically relevant quantities, this point in \mathcal{M} is, in fact, singular and should be blown up to resolve the singularity. For the generic dispersion relation the role of mass in above reasoning is played by the root \vec{k}_0^2 of the equation $\lambda_a(\omega = 0, \vec{k}_0^2) = 0$ (the real mass gap arises when the root is negative, $\vec{k}_0^2 < 0$). The DVZ jump can occur when $\vec{k}_0^2 \rightarrow -\infty$, and this actually requires that $\lambda_a(\omega = 0, \vec{k}^2)$ has an asymptote which satisfies (14). Thus, (14) is a necessary condition for a the DVZ jump to occur. Note, however, that (14) is more restrictive, because $\omega = 0$ condition is additionally imposed: thus it defines a codimension-one subspace in the moduli space \mathcal{M} , while (12) can hold for particular ω and \vec{k} in codimension-zero domains of \mathcal{M} . The DVZ jump is basically a non-commutativity of the limits, i.e. the difference between the two naive definitions of the static potential (the instantaneous Newton/Coulomb/Yukawa interactions) at a given point M_0 in the moduli space. Such a difference can occur when the number of degrees of freedom changes at M_0 , i.e. when the two branches of dispersion relations merge or intersect. This happens if the two roots $\lambda_a(\omega = 0, \vec{k})$ coincide, i.e. when (14) takes place.

In Appendix I we thoroughly study conditions of emergency of ghosts, tachyons, superluminals and the DVZ jumps in the example of massive vector theory.

6. Eigenvalues and discriminant analysis. The "eigenvalues" $\lambda_a(k)$ are roots of the characteristic polynomial

$$C_I(\lambda) = \text{discriminant}_\phi(S(\phi) - \lambda(\phi I \phi)) = \det(K - I\lambda) = \prod_a^{\text{deg } C} (\lambda - \lambda_a), \quad (19)$$

since the discriminant of a quadratic form is actually a determinant of the corresponding matrix. On-shell conditions $\lambda_a(k) = 0$ are zeroes of $\text{discriminant}_\phi(S(\phi)) = \det K$ itself and do not depend on the choice of I , as we already mentioned.

Similarly, conditions like (13) and (14) are zeroes of the ratio

$$\frac{\text{resultant}_\lambda(C(\lambda), \delta C(\lambda))}{\text{resultant}_\lambda(C(\lambda), C'(\lambda))} = (-1)^{1+\text{deg } C} \prod_a \delta \lambda_a \quad (20)$$

where δ is any variation of the coefficients of $C(\lambda)$, say, resulting from an infinitesimal change of ω^2 or \vec{k}^2 , and $C'(\lambda)$ is λ -derivative of $C(\lambda)$. Note that the resultant in the numerator has degree $\text{deg}(C) = \#(a)$ in the coefficients of δC , and the resultant in denominator is actually a discriminant of $C(\lambda)$. For definitions of resultants and discriminants see, e.g., [18, 19].

7. The pattern of eigenmodes for Lorentz-violating gravity. After these general remarks, we return to the concrete model: the linearized massive gravity (1).

Eigenvectors of the kinetic matrix are naturally split into three groups: traceless tensors, vectors and scalars. In more detail, the $\frac{d(d+1)}{2}$ components of symmetric tensor $h_{\mu\nu}$ are decomposed as follows:

$$\begin{aligned} \frac{d(d+1)}{2} &= \underbrace{\frac{(d-2)(d+1)}{2}}_{\text{massive spin 2}} + \underbrace{\frac{(d-1)}{\text{space-time transverse}} + \frac{1}{\text{secondary}} + \frac{1}{\text{space-time trace}}}_{\text{Stueckelberg vector}} = \quad (21) \\ &= \left\{ \underbrace{\frac{d(d-3)}{2}}_{\text{spatial-transverse tensor}} + \underbrace{\frac{(d-2)}{\text{longitudinal tensor}}}_{=\text{transverse vector}} + \frac{1}{\text{spatial trace}} \right\} + \left\{ \frac{d-2}{\text{spatial-transverse Stueckelberg vector}} + \frac{1}{\text{longitudinal Stueckelberg scalar}} + \frac{1}{\text{secondary Stueckelberg scalar}} \right\} + 1 \end{aligned}$$

where the first line is the $SO(d-1)$ classification in the rest frame (where $\vec{k} = 0$), while the second line is the classification in the arbitrary frame, i.e. that w.r.t. $SO(d-2)$, which acts in the hyperplane transverse to \vec{k} .

Accordingly the characteristic polynomial $C(\lambda)$ in the generic frame is decomposed as

$$C(\lambda) = (\lambda - \lambda_{gr})^{\frac{d(d-3)}{2}} P_2(\lambda)^{d-2} Q_4(\lambda) = (\lambda - \lambda_{gr})^{\frac{d(d-3)}{2}} (\lambda - \lambda_{vec}^+)^{d-2} (\lambda - \lambda_{vec}^-)^{d-2} \prod_{a=1}^4 (\lambda - \lambda_{sc}^a) \quad (22)$$

where P_2 and Q_4 are polynomials of degree 2 and 4 respectively and all their coefficients as well as λ_{gr} are quadratic functions of ω and \vec{k} . Since the coefficients of C are quadratic functions of ω and \vec{k} , this means that λ_{gr} is some bilinear combination of ω and \vec{k} ,

$$\lambda_{vec}^\pm = p_2 \pm \sqrt{p_4}, \text{ where } p_2 \text{ and } p_4 \text{ are respectively quadratic and quartic in } \omega \text{ and } \vec{k},$$

$$\lambda_{sc}^{1,2,3,4} \text{ are the roots of degree-four polynomial.}$$

In the rest frame the roots should be grouped in a different way, according to the first line in (21)

$$C_{RF}(\lambda) = (\lambda - \lambda_{gr})^{\frac{(d-2)(d+1)}{2}} (\lambda - \lambda_{vec})^{d-1} (\lambda - \lambda_{sc}^+) (\lambda - \lambda_{sc}^-) \Big|_{\vec{k}=0} = 0 \quad (23)$$

i.e. at $\vec{k} = 0$

$$\begin{aligned} \lambda_{vec}^+(\vec{k} = 0) &= \lambda_{gr}(\vec{k} = 0), \\ \lambda_{sc}^{spT}(\vec{k} = 0) &= \lambda_{gr}(\vec{k} = 0), \\ \lambda_{sc}^{spS}(\vec{k} = 0) &= \lambda_{vec}^-(\vec{k} = 0) \end{aligned} \quad (24)$$

where "spT" and "spS" label the spatial trace h_{ii} and the spatial Stueckelberg scalar $h_{0i} = k_i s$ respectively. The remaining two scalars, the space-time trace (stT) h_μ^μ and the secondary Stueckelberg scalar (seS) $h_{\mu\nu} = k_\mu k_\nu \sigma$ have eigenvalues, which are roots of quadratic equation:

$$\lambda_{sc}^\pm = q_2 \pm \sqrt{q_4} \Big|_{\vec{k}=0} \quad (25)$$

In Lorentz invariant theory one can obtain eigenvectors and eigenvalues in an arbitrary frame by a Lorentz boost, but Lorentz violation forbids such a simple procedure.

In gauge invariant theory all the d Stueckelberg fields have vanishing eigenvalues and one gets

$$C_{GI}(\lambda) = \lambda^d (\lambda - \lambda_{gr})^{\frac{d(d-3)}{2}} (\lambda - \lambda_{vec}^+)^{d-2} (\lambda - \lambda_{sc}^{spT}) (\lambda - \lambda_{sc}^{stT}) \quad (26)$$

i.e. in this case the two trace (spT and spS) eigenvalues are the roots of quadratic equation,

$$\lambda_{sc}^{\pm T} = t_2 \pm \sqrt{t_4} \Big|_{GI} \quad (27)$$

Actually gauge invariant will be only the massless gravity (where, by the way, transition to the rest frame is not a justified operation). This can be summarized in the following scheme:

| rest frame | | normal modes | | gauge invariant (massless) case |
|-------------------------------|---------------|-------------------------------|---|---------------------------------|
| | | graviton | → | graviton |
| massive graviton | ↙ ← ⊕ ↘ | | | |
| | | vector | → | vector |
| Stueckelberg $(d-1)$ -vector | ↙ ↘ | Stueckelberg vector | ↘ | Stueckelberg d -vector |
| | | Stueckelberg scalar | → | |
| secondary Stueckelberg scalar | ← | secondary Stueckelberg scalar | ↗ | |
| | ⊕ ← | spatial trace | → | spatial trace |
| space-time trace | ← | space-time trace | → | space-time trace |

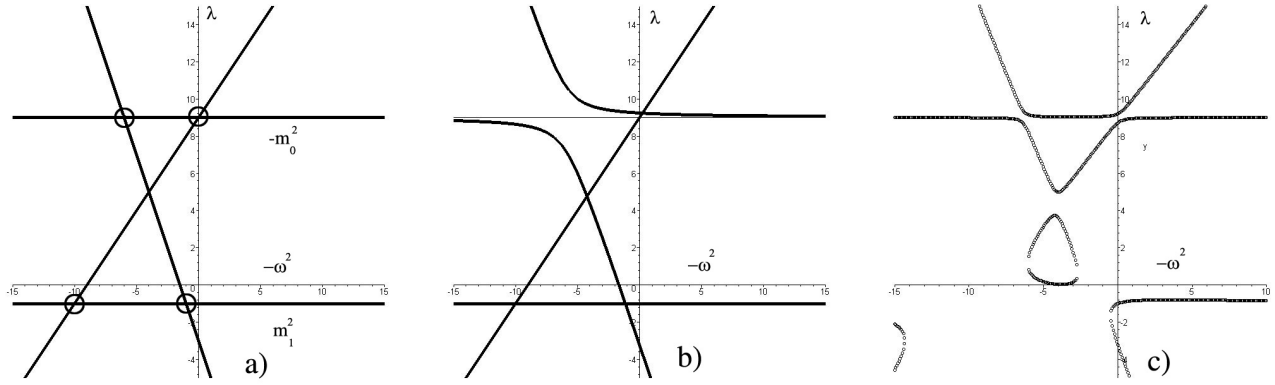


Figure 1: The left picture plots the four eigenvalues as functions of $-\omega^2$ in the Lorentz-non-invariant case in the rest frame and with $m_4 = 0$. In this case, the figure is maximally degenerated, and all the eigenvalues are straight lines. The pattern is described by positions of the two horizontal lines given by values of m_0^2 and m_1^2 , and by positions of the four intersections which depend also on m_2^2 and m_3^2 . In the middle figure, the degeneration is partly lifted by choosing non-zero m_4 (still in the rest frame). At last, in the right figure, a typical perturbation of the previous figures shown, when both non-zero m_4^2 and momentum are switched on resolving all the four marked crossings of the left figure. The parameters here are: $m_0^2 = -9$, $m_1^2 = -1$, $m_2^2 = 9$, $m_3^2 = 4$.

The most interesting sector is that of scalars, with complicated inter-mixture of four eigenvectors. The pattern of eigenvalues is most simple at $m_4 = 0$ and $\vec{k} = 0$:

$$\begin{aligned}
 \lambda_{sT} &= -\omega^2 + m_2^2, \\
 \lambda_S &= m_1^2, \\
 \lambda_{sS} &= -m_0^2, \\
 \lambda_{stT} &= (d-2)\omega^2 + m_2^2 - (d-1)m_3^2
 \end{aligned} \tag{28}$$

see Fig.1a.

Switching on m_4 and \vec{k} leads to a bifurcation: repulsion of levels, so that Fig.1a is immediately transformed into Fig.1b. What is important, however, the horizontal asymptotes stay at their positions: at $\lambda = -m_0^2$ and $\lambda = m_1^2$.

Bifurcations become visible in the physical spectrum when one of these asymptotes coincide with the real axis, $\lambda = 0$. Clearly, this happens when either $m_0 = 0$ or $m_1 = 0$.

In this paper we introduce eigenvalues in a Lorentz-invariant way, taking $I = I_L = \eta = \text{diag}(-1, 1, \dots, 1)$, even despite the Lorentz symmetry can be explicitly violated by mass terms in the Lagrangian. This should be kept in mind in comparison to [14], where "Euclidean" eigenvalues were considered, associated with the choice $I = I_E = \text{diag}(1, 1, \dots, 1)$ (see also Appendix II).

8. Restriction to subspace of Lorentz invariant theories in \mathcal{M} . To reveal the physical meaning of pictures like Fig.1, it is instructive to begin with the simpler Lorentz-invariant case (2) with only two moduli A and B . In this model the Lorentz symmetry expresses eigenvalues in arbitrary frame through those in the rest frame, so that the classification of eigenvectors is always described by the left column of the table. It remains only to evaluate concrete functions of $k^2 = -\omega^2 + \vec{k}^2$:

| | | | |
|---------------------|----------------|--|------|
| tensors | $(d+1)(d-2)/2$ | $\lambda_{gr} = k^2 + A$ | |
| Stueckelberg vector | $d-1$ | $\lambda_{vec} = A$ | (29) |
| scalars | 2 | $\lambda_{sc}^\pm = A - \frac{(d-2)k^2 + dB \pm \sqrt{(d-2)^2(k^2+B)^2 + 4(d-1)B^2}}{2}$ | |

Thus in the Lorentz invariant case we have two scalars: the space-time trace ("+" sign in above formula) and the secondary Stueckelberg ("-" sign). When the Lorentz invariance is violated, we will get 4 scalars, two additional coming from the tensor and vector multiplets (the spatial trace and spatial Stueckelberg scalar respectively). In Fig.2 we plot eigenvalues corresponding to these four scalars as functions of k^2 in the Lorentz invariant case (we include those two scalars that are parts of the tensor and vector multiplets in this case). The parameter A enters as a common shift of the horizontal axis, and the mass-shell condition $\lambda = 0$ for propagating particles is satisfied at the intersections of the eigenvalue curves in the picture with the abscissa axis. We see that the four lines become straight, like in Fig.1a, only at $B = 0$, Fig.2c: this is the only point where the condition $m_4 = 0$ is consistent with (2). For finite B , the two eigenvalues λ_{sc} are repulsed, like in Fig.1b, while nothing happens

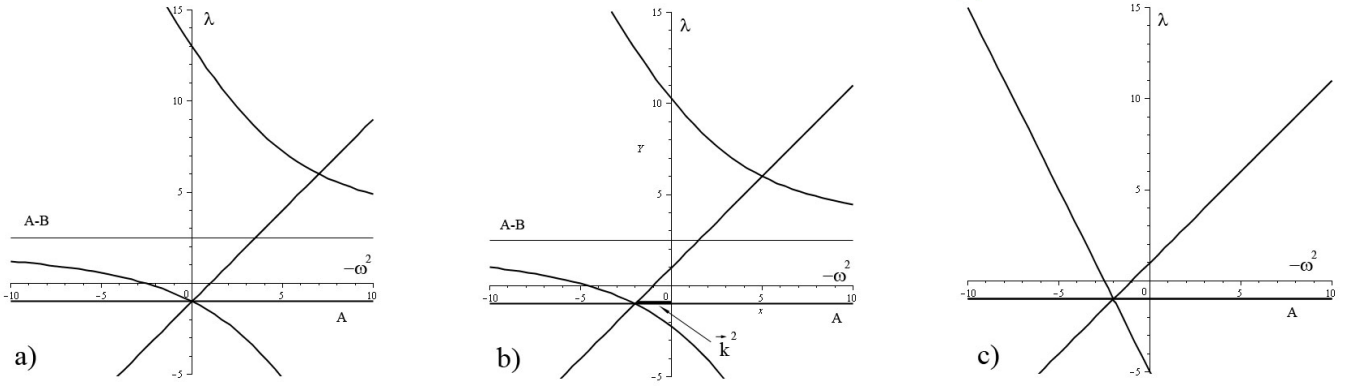


Figure 2: The left figure plots the four eigenvalues in the Lorentz-invariant case at zero momentum, and the middle figure at non-zero momentum (which corresponds just to shifting the whole figure to the left). The right figure corresponds to the degenerated case of $B = 0$. **Note that in this case there is no way to resolve all the intersections of the right picture.**

to the other two eigenvalues, protected by the Lorentz symmetry: only two scalars can mix in this symmetric situation.

We see that of these two scalars only one can be on-shell and, whatever it is, it is a ghost, see (12): the slope of the curve $\lambda(-\omega^2)$ is negative everywhere and thus also on mass-shell, where $\lambda(-\omega^2) = 0$. It is a tachyon or not, depending on where the intersection with the abscissa axis occurs: to the right (tachyon) or to the left (normal) of the ordinate axis (for positive or negative $k^2 = -\omega^2 + \vec{k}^2$). The only chance for this ghost to disappear from the spectrum of propagating particles is when the thin line (asymptotics of the eigenvalues) coincides with the abscissa axis, i.e. when $A = B$: this is exactly the Pauli-Fierz model [1]. Clearly, at this point (13) is fulfilled. However, exactly at the same point in the moduli space condition (14) is also satisfied, and the DVZ jump occurs (it comes with no surprise, because (13) and (14) always coincide if the Lorentz invariance is not violated).

The DVZ jump occurs because the instantaneous-interaction potential $V(\vec{k}) = \Pi(\omega = 0, \vec{k})$ does not have a well defined limit when both A and B tend to zero. Instead, $V(\vec{k})$ is well defined on a properly compactified moduli space with a blown-up singularity at $A = B = 0$: if one parameterize B as $B = A + A^2\xi$, then V is actually a smooth function of A and ξ , see Fig.3c. In more detail, the Newton/Yukawa-potential is given by

$$V(k) = \frac{J_0(k)J_0(k)}{(d-1)(d-2)} \left(\frac{d-2}{k^2 + m^2} + \frac{1}{k^2 + M^2} \right), \quad m^2 = A, \quad M^2 = \frac{A(dB - A)}{(d-2)(A - B)} \quad (30)$$

see [14, s.3.6]. It is plotted as a function of A and B in Fig.3a at some fixed value of k^2 . Poles at the two lines $k^2 + m^2 = 0$ and $k^2 + M^2 = 0$ correspond to propagating degrees of freedom, the second singularity may exist even at $\omega^2 = 0$ i.e. at positive k^2 , because the ghost can be also a tachyon, with $M^2 < 0$ (it is *not* the case if $B \leq A \leq dB$). Clearly, the function V is discontinuous at $A = B = 0$, but the singularity is resolved in the coordinates (A, ξ) in Fig.3c, at expense of gluing in a whole line ($A = 0, \xi$) instead of a single point $A = B = 0$ (the singularity point is "blown up"). The situation is of course similar to the resolution of the singularity at $A = B = 0$ in the rational function $\frac{A-B}{A+B}$ by passing, say, to polar or non-homogeneous coordinates $B = A\xi'$, the difference here is that the singularity in (30) is rather cusp-like, see Fig.3b, and the blow-up procedure is slightly more involved.

9. Back to generic Lorentz violating theory. Coming back to the Lorentz-violating masses (1), we obtain a somewhat richer pattern of bifurcations, but their physical interpretations remain very similar. The essentially new thing is that the singular subspace of the moduli space has higher codimension and can be passed by in an easier way.

We begin with the analogue of Fig.2a in the rest frame: see Fig.1b. To keep pictures similar to the Lorentz-invariant case, we plot dependencies on $-\omega^2$, not $+\omega^2$. Instead of (29), we have now

| | | | |
|---------------------|------------------------|--|------|
| tensors | $\frac{(d+1)(d-2)}{2}$ | $\lambda_{gr} = -\omega^2 + m_2^2$ | |
| Stueckelberg vector | $d - 1$ | $\lambda_{vec} = m_1^2$ | (31) |
| scalars | 2 | $\lambda_{sc}^{\pm} = \frac{m_2^2 - m_0^2 - (d-1)m_3^2 + (d-2)\omega^2 \pm \sqrt{\left(m_2^2 + m_0^2 - (d-1)m_3^2 + (d-2)\omega^2\right)^2 + 4(d-1)m_4^4}}{2}$ | |

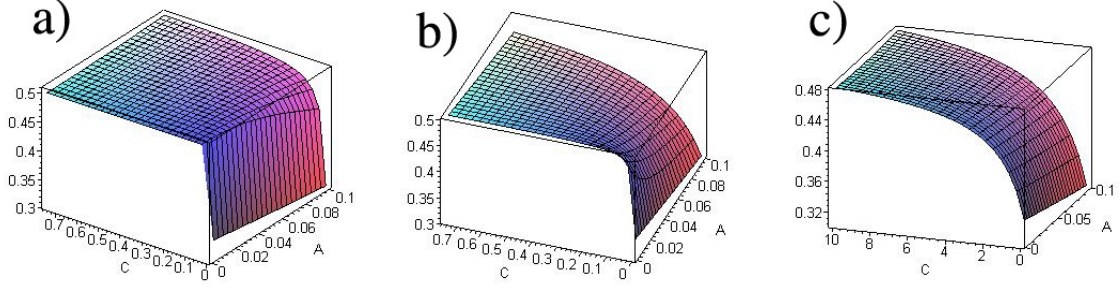


Figure 3: Resolution of singularity in potential V at $A = B = 0$. Plotted are potentials V at $k^2 = 1$ as functions of A and C , where C substitutes B and is introduced in three different ways: $B = A + C$ (Fig.a), $B = A + AC$ (Fig.b), $B = A + A^2C$ (Fig.c). Clearly, V is a smooth function at $A = 0$ only in the third case. Of course, V is also singular when propagating particles contribute, i.e. at $k^2 + m^2 = 0$ and $k^2 + M^2 = 0$. These singularities are avoided since we present only a fragment of plots with small enough $A \ll k^2 = 1$.

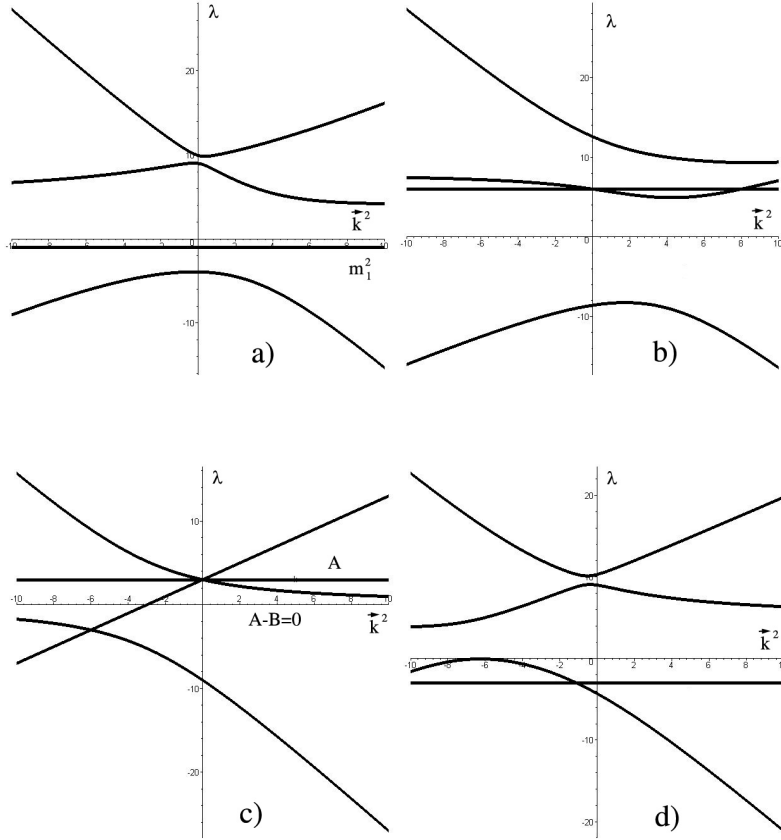


Figure 4: The eigenvalue curves at $\omega^2 = 0$ (which are relevant to describing the potential). The first two figures (a and b) correspond to the generic Lorentz violating case (the values of parameters are $m_0^2 = -9$, $m_1^2 = -1$, $m_2^2 = 9$, $m_3^2 = 4$, $m_4^2 = -2$ and $m_0^2 = 8$, $m_1^2 = m_2^2 = 6$, $m_3^2 = m_4^2 = -2$). The third figure (c) describes the Lorentz invariant case, when the eigenvalue asymptotics coincide with the abscissa axis. This corresponds to the DVZ jump and, at the same time, to the Pauli-Fierz theory ($A = B = 3$). Figure d ($m_0^2 = -9$, $m_1^2 = -3$, $m_2^2 = 9$, $m_3^2 = 4$, $m_4^2 = 2.4$) demonstrates that condition (14) can be also realized in a different way (when one of the eigenvalue curve touches the abscissa axis).

Of the four crossings at $P1, P2, P3, P4$ in Fig.1a no one is protected by the Lorentz invariance, still in the rest frame only one is resolved by switching on $m_4 \neq 0$, Fig.1b. The remaining crossings are resolved when we also switch on non-vanishing \vec{k}^2 , then

$$\begin{array}{lll}
\text{tensors} & \frac{d(d-3)}{2} & \lambda_{gr} = -\omega^2 + \vec{k}^2 + m_2^2 \\
\text{vectors} & 2 \times (d-2) & \lambda_{vec}^\pm = \frac{-\omega^2 + \vec{k}^2 + m_1^2 + m_2^2 \pm \sqrt{(-\omega^2 + \vec{k}^2)^2 + 2(m_1^2 - m_2^2)(\omega^2 + \vec{k}^2) + (m_1^2 - m_2^2)^2}}{2} \\
\text{scalars} & 4 & C_4(\lambda_{sc}) = 0
\end{array} \tag{32}$$

where the polynomial C_4 of degree 4 in λ is explicitly presented in Appendix III, eq.(73). The result is shown in Fig.1c. In these pictures, the on-shell conditions for propagating particles correspond to intersections with the abscissa axis. Propagating particles disappear from the spectrum when this axis coincides with one of the eigenvalue asymptotics (thin lines in figures).

In order to investigate the DVZ jumps in the instantaneous-interaction potential, one should instead look at Fig.4, where the four scalar λ 's are plotted as functions of \vec{k}^2 at vanishing ω^2 . Any crossing with the abscissa axis in this picture corresponds to a tachyon. The DVZ jumps occur when any of the eigenvalue asymptotics (thin lines) coincide with the abscissa axis. For more pictures, describing the emerging phases, see Appendix IV.

10. Conserved currents and instantaneous interaction. In gauge-invariant theories the currents, attached to the gauge field in (4), are conserved: if not imposed "by hands", this condition appears automatically from integration over the pure gauge degrees of freedom. When the gauge invariance is explicitly broken, say, by the mass terms in the second line of (1), this requirement is no longer enforced by the theory itself, instead it is imposed on massive gravity on phenomenological grounds: according to the currently dominating paradigm one is allowed to "spoil" properties of the gravity sector, but not of the matter one, which is believed to be under a much better experimental control.

Conservation of currents is extremely important, because it *de facto* eliminates some would-be propagating degrees of freedom from the physically relevant quantity $\Pi(k)$. Let us remind that in ordinary photodynamics, i.e. the Maxwell theory with Lagrangian $F_{\mu\nu}^2$, we have $\Pi = \frac{J_\mu J^\mu}{\omega^2 - \vec{k}^2}$ what is actually equal to

$$\Pi = \frac{J_\perp^2}{\omega^2 - \vec{k}^2} + \frac{J_0^2}{\vec{k}^2} \tag{33}$$

for conserved current, satisfying $\omega J_0 = \vec{k} \vec{J} = |\vec{k}| J_\parallel$, so that the longitudinal photon is actually eliminated from Π , being substituted by a non-propagating instant Coulomb interaction. This fact persists in other theories with conserved currents, including (1), even if the gauge symmetry is violated by mass terms: the Coulomb interaction becomes the Yukawa one or even more complicated but continue to possess an instantaneous component. However, this is not explicitly seen at the level of eigenvalue analysis that we performed in this paper. This "drawback" can probably be cured by considering the "Euclidean eigenvalues", suggested in [14], but this can also be considered as a rather artificial trick.

Another important remark is that even if some mode drops away from Π when the currents are conserved, this by no means implies it can not be *radiated* (emitted) by a conserved current: one can easily imagine situations (construct models) when a mode is emitted, but can not be captured by another conserved current later. This happens if space-time transverse modes are mixed with the pure gauge ones – what can not be generically forbidden in gauge-violating theories. If this happens, then the fact that the mode drops away from Π is not sufficient to claim that it is indeed non-propagating, and one should be careful and not overlook such possibility.

11. Conclusion. To conclude, we used the currently popular example of linearized massive gravity [3] to illustrate the general behavior of normal modes (quasiparticles) over moduli spaces of sophisticated physical theories and proposed to analyze this behavior by the standard techniques of linear and non-linear algebra [19]. Already in this relatively simple example we observe a rich pattern of bifurcations and a need to resolve singularities in the moduli space in order to avoid the DVZ discontinuities [9] and other pathologies. This simple exercise can serve as an elementary introduction to the general string theory problems from the perspective of ordinary – and even phenomenologically acceptable – classical field theory. At the same time, this analysis can help to visualize and systematize the results of [3] about the ghost-free versions of massive gravity and further clarify role of the Lorentz violation in constructing such a theory, at least, at the level of quadratic approximation. Whatever will be its relevance for phenomenological application, massive gravity looks very convenient for fighting prejudices of previous experience, unapplicable when the gauge and Lorentz invariances

are broken, and it will play a role in building new bridges between elementary particle physics and generic quantum field/string theory.

Acknowledgements

We are indebted for hospitality and support to Prof.T.Tomaras and the Institute of Theoretical and Computational Physics of University of Crete during the summer of 2008, where this work was done. We are specially grateful to T.Tomaras for interest, long discussions and collaboration. We are also indebted to T.Mironova for help with the pictures.

Our work is partly supported by Russian Federal Nuclear Energy Agency, by the joint grants 09-02-91005-ANF and 09-01-92440-CE, by the Russian President's Grants of Support for the Scientific Schools NSh-3035.2008.2 (A.Mir.,Al.Mor.) and NSh-3036.2008.2 (S.Mir.,An.Mor.), by RFBR grants 07-02-00878 (A.Mir.), 08-02-00287 (S.Mir.), 07-02-00645 (Al.Mor.) and 07-01-00526 (An.Mor.).

References

- [1] M.Fierz, *Helv.Phys.Acta* **12** (1939) 3
M.Fierz and W.Pauli, *Proc.Roy.Soc.* **173** (1939) 211
- [2] A.Logunov, *Relativistic Theory of Gravity*, Commack, USA: Nova Sci. Publ. (1998) 114 p.
G.t'Hooft, arXiv:0708.3184 [hep-th]
- [3] V.Rubakov, hep-th/0407104
S.Dubovsky, *JHEP* **0410** (2004) 076 (hep-th/0409124)
S.Dubovsky, P.Tinyakov and I.Tkachev, *Phys.Rev.Lett.* **94** (2005) 181102 (hep-th/0411158); *Phys.Rev.* **D72** (2005) 084011 (hep-th/0504067)
V.Rubakov and P.Tinyakov, *Phys.Usp.* **51** (2008) 759-792, arXiv:0802.4379
- [4] N.Arkani-Hamed, H.Georgi and M.D.Schwartz, *Ann.Phys.* **305** (2003) 96 (hep-th/0210184)
M.Porrati, *JHEP* **04** (2002) 058 (hep-th/0112166)
- [5] See, e.g., the review:
P.J.E.Peebles and B.Ranta, *Rev.Mod.Phys.* **75** (2003) 559, astro-ph/0207347 and references therein
- [6] For example, the DVZ jump is absent in AdS, see:
I.I. Kogan, S. Mouslopoulos, A. Papazoglou and L. Pilo. *Nucl. Phys.* **B625** (2002) 179, hep-th/0105255;
Phys. Lett. **B503** (2001) 173, hep-th/0011138
M. Porrati. *Phys. Lett.* **B498** (2001) 92, hep-th/0011152
A. Karch, E. Katz and L. Randall. *JHEP* **0112** (2001) 016, hep-th/0106261
P.A.Grassi and P. van Nieuwenhuizen, *Phys.Lett.* **B499** (2001) 174-178 0011278
Y.S.Myung, hep-th/0012082
For other aspects and references see
M.Novello and R.P.Neves, *Class.Quantum Grav.* **20** (2003) L67-L73
- [7] J.Bekenstein, *Phys.Lett.* **B202** (1988) 497; *Phys.Rev.* **D70** (2004) 083509, astro-ph/0403694; *PoS JHW2004* (2005) 012, astro-ph/0412652
- [8] A.Vainshtein, *Phys.Lett.* **B39** (1972) 393
- [9] H. van Dam and M.J.C.Veltman, *Nucl.Phys.* **B22** (1970) 397
V.I.Zakharov, *JETP Lett.* **12** (1970) 312
- [10] P.van Nieuwenhuizen, *Nucl.Phys.* **B60** (1973) 478-492
- [11] D.G.Boulware and S.Deser, *Phys.Rev.* **D4** (1972) 3368
- [12] J.Bjorken, *Ann.Phys.* **24** (1963) 174, see also hep-th/0111196
S.Coleman, S.Glashow, *Phys.Rev.* **D59** (1999) 116008 hep-ph/9812418
V.A.Kosteletzky and S.Samuel, *Phys.Rev.***D39** (1989) 683
V.A.Kosteletzky and R.Potting, *Nucl.Phys.* **B359** (1991) 545
D.Colladay and V.A.Kosteletzky, *Phys.Rev.* **D55** (1997) 6760; *Phys.Rev.* **D58** (1998) 116002
J. W. Moffat, *Int. J. Mod. Phys. D* **12** (2003) 1279 , hep-th/0211167
D. Colladay, *AIP Conf. Proc.* **672** (2003) 65, hep-ph/0301223

- O. Bertolami, R. Lehnert, R. Potting, A. Ribeiro, Phys. Rev. D **69** (2004) 083513, astro-ph/0310344
 S. M. Carroll and E. A. Lim, Phys. Rev. D **70** (2004) 123525, hep-th/0407149
 O. Bertolami and J. Paramos, Phys. Rev. D **72** (2005) 044001, hep-th/0504215
 R. Bluhm and V. A. Kostelecky, Phys. Rev. D **71** (2005) 065008, hep-th/0412320
 R. Bluhm, Lect. Notes Phys. **702** (2006)191, hep-ph/0506054; Int. J. Mod. Phys. D **16** (2008) 2357, hep-th/0607127; arXiv:0801.0141
 P. G. Ferreira, B. M. Gripaios, R. Saffari and T. G. Zlosnik, Phys. Rev. D **75** (2007) 044014, astro-ph/0610125
 M. Gomes, T. Mariz, J. R. Nascimento and A. J. da Silva, Phys. Rev. D **77** (2008) 105002, arXiv:0709.2904
 Arianto, F. P. Zen, B. E. Gunara, Tryanta and Supard, JHEP **09** (2007) 048, arXiv:0709.3688
 J. W. Moffat and V. T. Toth, arXiv:0710.0364
 R. Bluhm, S. H. Fung and V. A. Kostelecky, Phys. Rev. D **77** (2008) 065020, arXiv:0712.4119
 V. A. Kostelecky and N. Russell, arXiv:0801.0287
 S. M. Carroll, arXiv:0802.0521
 R. Bluhm, N. L. Gagne, R. Potting and A. Vrublevskis, Phys. Rev. D **77** (2008) 125007, arXiv:0802.4071
 L. Grisa, arXiv:0803.1137
 R. Obousy and G. Cleaver, arXiv:0805.0019
 T.Mariz, J.Nascimento, A.Petrov, A.Santos and A.da Silva, *Spontaneous Lorentz symmetry breaking and cosmological constant*, arXiv:0807.4999
 Z.Berezhiani and O.Kancheli, arXiv:0808.3181
 E.Kiritsis and V.Niarchos, arXiv:0808.3410
- [13] P.Horava, arXiv:0901.3775; arXiv:0902.3657
- [14] A.Mironov, S.Mironov, A.Morozov and And.Morozov, arXiv:0910.5243 (hep-ph)
- [15] A.Morozov, Sov. Phys. Usp. **35** (1992) 671-714
- [16] A.Morozov, Phys.Usp.(UFN) **37** (1994) 1, hep-th/9303139; hep-th/9502091; hep-th/0502010
 A.Mironov, Int.J.Mod.Phys. **A9** (1994) 4355, hep-th/9312212; Phys.Part.Nucl. **33** (2002) 537
 A.Gerasimov, S.Khoroshkin, D.Lebedev, A.Mironov, and A.Morozov, Int.J.Mod.Phys. A10 (1995) 2589-2614, hep-th/9405011
 A.Mironov, A.Morozov, and L.Vinet, Theor.Math.Phys. **100** (1995) 890-899, hep-th/9312213
 S.Kharchev, A.Mironov, and A.Morozov, Theor.Math.Phys. **104** (1995) 129-143, q-alg/9501013
 A.Mironov, hep-th/9409190; Theor.Math.Phys. **114** (1998) 127, q-alg/9711006
- [17] Superluminal propagation in general relativity was discussed in:
 A.D.Dolgov and I.B.Khrplovich, Phys.Lett. **A243** (1998) 117, hep-th/9708056
 S.Liberati, S.Sonogo and M.Visser, Annals Phys. **298** (2002) 167, gr-qc/0107091
 For spectacular fresh analysis of this subject see the recent papers:
 T.J.Hollowood and G.M.Shore, Phys.Lett. **B655** (2007) 67, arXiv:0707.2302; Nucl.Phys. **B795** (2008) 138, arXiv:0707.2303; JHEP **0812** (2008) 091, arXiv:0806.1019
- [18] B.L.Van der Waerden, *Algebra* I, II (Springer-Verlag, 1967, 1971)
 S.Lang, *Algebra*, Springer
- [19] V.Dolotin and A.Morozov, *Introduction to Non-Linear Algebra*, World Scientific, 2007 (hep-th/0609022); *Universal Mandelbrot Set. Beginning of the Story*, World Scientific, 2006 (hep-th/0501235);
 Int.J.Mod.Phys. **A23** (2008) 3613-3684, hep-th/0701234
 And.Morozov, JETP Lett. **86** (2007) 745-748, arXiv:0710.2315
 Sh.Shakirov and A.Morozov, arXiv:0804.4632; arXiv:0807.4539; arXiv:0903.2595
 A.Anokhina, A.Morozov and Sh.Shakirov, arXiv:0812.5013

Appendix I. Breaking Lorentz invariance in vector theory

Here we consider the theory of massive vector field with the Lorentz invariance manifestly broken.

Euclidean eigenvalues

If one chooses the unit (Euclidean) matrix for I in (8), one has to diagonalize the following kinetic operator:

$$K_{\mu\nu} = \begin{pmatrix} k_{\parallel}^2 + M_0^2 & \omega k_{\parallel} & 0 \\ \omega k_{\parallel} & \omega^2 - M_1^2 & 0 \\ 0 & 0 & \omega^2 - (k_{\parallel}^2 + M_1^2) \end{pmatrix} \quad (34)$$

where the spatial momentum, k_{\parallel} is directed along the first direction and $M_{0,1}$ are the massive terms that manifestly break the Lorentz invariance. The problem of diagonalizing this matrix leads to Euclidean eigenvalues, the result reads:

$$\lambda_- = \frac{1}{2} \left(\Delta - \sqrt{\Delta^2 - 4(M_0^2\omega^2 - M_1^2k_{\parallel}^2 - M_0^2M_1^2)} \right) \quad (35)$$

$$\lambda_+ = \frac{1}{2} \left(\Delta + \sqrt{\Delta^2 - 4(M_0^2\omega^2 - M_1^2k_{\parallel}^2 - M_0^2M_1^2)} \right) \quad (36)$$

with

$$\Delta = \omega^2 + k_{\parallel}^2 + M_0^2 - M_1^2 \quad (37)$$

and all other $d - 2$ eigenvalues are equal to

$$\lambda_i = \omega^2 - k_{\parallel}^2 - M_1^2 \quad (38)$$

There are two kinds of dispersion laws. The condition $\lambda_i = 0$ evidently leads to the $d - 2$ excitations with the dispersion law

$$\omega^2 = k_{\parallel}^2 + M_1^2 \quad (39)$$

At the same time, the conditions $\lambda_{\pm} = 0$ have only one solution

$$\omega^2 = M_1^2 + \frac{M_1^2}{M_0^2} k_{\parallel}^2 \quad (40)$$

The simplest way to see this is to look at the determinant of $K_{\mu\nu}$ which is equal to

$$\left(\omega^2 - k_{\parallel}^2 - M_1^2 \right)^{d-2} \left(-M_0^2\omega^2 + M_0^2M_1^2 + M_1^2k_{\parallel}^2 \right) \quad (41)$$

Now one can easily analyze these eigenvalues for physical effects:

tachyons: Dispersion law (39) leads to a tachyon as soon as $M_1^2 < 0$. At the same time, dispersion law (40) leads to a tachyon when $M_0^2 < 0$.

superluminal: This may come only from dispersion law (40), which always violates Lorentz invariance unless $M_0^2 = M_1^2$ (since then some of the vector field modes propagate with the speed of light, and some with the speed of light times M_1/M_0), and, in the case of $M_1/M_0 > 1$, describes the superluminal.

ghosts: The ghost content of the theory is controlled by the derivatives $\frac{\partial\lambda}{\partial\omega^2}$ on mass shell (i.e. at points, where $\lambda = 0$). These are

$$\frac{\partial\lambda_i}{\partial\omega^2} = 1 \quad (42)$$

and

$$\frac{\partial\lambda_-}{\partial\omega^2} = \frac{M_0^4}{k_{\parallel}^2(M_0^2 + M_1^2) + M_0^4} \quad (43)$$

This derivative is zero only when M_0^2 . However, the ghost content of the theory can not change at this point, since it is M_0^4 that enters the numerator and the ghost never emerges. If, however, $M_0^2 + M_1^2 < 0$, there is also a singular point where the derivative changes the sign and, therefore, the ghost emerges.

The condition $M_0 = 0$ is a counterpart of the condition $m_0 = 0$ in the gravity case, in this case the "live" excitation branch comes away from the spectrum. Another special case is $M_1 = 0$ when there only constant (in space) mode is present in the spectrum. This is an analog of the $m_1 = 0$ condition in gravity.

DVZ jump: It is described by the derivatives $\frac{\partial \lambda}{\partial k_{\parallel}^2}$ at zero frequencies. The derivatives are

$$\frac{\partial \lambda_i}{\partial k_{\parallel}^2} = -1 \quad (44)$$

and

$$\frac{\partial \lambda_{\pm}}{\partial k_{\parallel}^2} = \begin{pmatrix} 0 \\ 1 \end{pmatrix} \quad (45)$$

Therefore, one of the derivatives is zero and, hence, there can be a DVZ jump.

DVZ jump

We obtained that the necessary condition of the DVZ jump requiring that (45) to be zero is fulfilled. However, it is identical zero for all values of parameters which makes the general argument about the DVZ condition meaningless⁵. Therefore, to establish if the DVZ jump is realized, one needs a closer inspection of the interaction. The interaction with external currents is given by the term $JK^{-1}J$ in the action, where J is a column $(J_0, J_{\parallel}, J_{\perp})$ and the propagator is the inverse of K (34). If one additionally requires for the currents to be conserved, $\frac{\partial J^{\mu}}{\partial x^{\mu}} = 0$, the interaction reads

$$\frac{J_0^2}{k_{\parallel}^2} \frac{k_{\parallel}^2 M_1^2 - \omega^2 M_0^2}{k_{\parallel}^2 M_1^2 - \omega^2 M_0^2 + M_0^2 M_1^2} + \frac{J_{\perp}^2}{\omega^2 - k_{\parallel}^2 - M_1^2} \quad (46)$$

Bringing masses to zero in this expression in any order, as well as putting them first equal (the Lorentz-invariant case) and then bringing to zero leads to the same result reproducing the standard QED

$$\frac{J_0^2}{k_{\parallel}^2} + \frac{J_{\perp}^2}{\omega^2 - k_{\parallel}^2} \quad (47)$$

If one consider a static potential in (46), i.e. the interaction generated by a static external current, $J_{\perp} = 0$ with $\omega = 0$, one obtains

$$\frac{J_0^2}{k_{\parallel}^2} \frac{k_{\parallel}^2}{k_{\parallel}^2 + M_0^2} \quad (48)$$

which also does not shows up any jumps. Therefore, there is no the DVZ jump in this case.

This is mostly due to a specific form of the interaction. Would be there a term, e.g., M_0^4 instead of $M_0^2 M_1^2$ in the denominator of (46), there is the DVZ jump. Moreover, would one consider not the static potential, but instead the case when $\omega = k_{\parallel}$ (with J_{\perp} still zero), the limits of (46) would be different for different ways of bringing masses to zero:

$$\left\{ \begin{array}{ll} \frac{J_0^2}{k_{\parallel}^2} & \text{if first } M_0 \rightarrow 0 \text{ (coincides with the massless QED case)} \\ -\frac{J_0^2}{k_{\parallel}^2} & \text{if first } M_1 \rightarrow 0 \\ 0 & \text{if first } M_0 = M_1 \end{array} \right. \quad (49)$$

Lorentz eigenvalues

The other possible choice of the matrix I in (8) is the Lorentzian unit matrix, which means in the case under consideration that one has to diagonalize the kinetic operator

$$K_{\nu}^{\mu} = \begin{pmatrix} -k_{\parallel}^2 - M_0^2 & -\omega k_{\parallel} & 0 \\ \omega k_{\parallel} & \omega^2 - M_1^2 & 0 \\ 0 & 0 & \omega^2 - (k_{\parallel}^2 + M_1^2) \end{pmatrix} \quad (50)$$

⁵It sounds as follows. Suppose one considers the static potential at small values of mass parameters. Then, if the coefficient in front of k_{\parallel}^2 in the denominator of the propagator (=an eigenvalue) is not going to zero with mass, nothing drastical happens. If, however, it goes to zero, one needs some further inspection of the situation.

Diagonalizing this matrix leads to the Lorentz eigenvalues, the result reads:

$$\lambda_-^L = \frac{1}{2} \left(\Delta_L - \sqrt{\Delta_L^2 + 4(M_0^2 \omega^2 - M_1^2 k_{\parallel}^2 - M_0^2 M_1^2)} \right) \quad (51)$$

$$\lambda_+^L = \frac{1}{2} \left(\Delta_L + \sqrt{\Delta_L^2 + 4(M_0^2 \omega^2 - M_1^2 k_{\parallel}^2 - M_0^2 M_1^2)} \right) \quad (52)$$

with

$$\Delta_L = \omega^2 - k_{\parallel}^2 - M_0^2 - M_1^2 \quad (53)$$

and all other $d - 2$ eigenvalues are equal to

$$\lambda_i^L = \omega^2 - k_{\parallel}^2 - M_1^2 \quad (54)$$

There are again the same two kinds of dispersion laws,

$$\omega^2 = k_{\parallel}^2 + M_1^2 \quad (55)$$

and

$$\omega^2 = M_1^2 + \frac{M_1^2}{M_0^2} k_{\parallel}^2 \quad (56)$$

since the determinant

$$\det K_{\nu}^{\mu} = \det \eta^{\mu\rho} \det K_{\rho\nu} = -\det K_{\mu\nu} \quad (57)$$

Now one can again analyze the eigenvalues for physical effects:

tachyons: Since the dispersion laws are the same, the tachyon also emerge under the same conditions as in the Euclidean case.

superluminal: Similarly, the condition for superluminals to emerge are the same.

ghosts: The derivatives $\frac{\partial \lambda}{\partial \omega^2}$ on mass shell for the Lorentz eigenvalues are

$$\frac{\partial \lambda_i^L}{\partial \omega^2} = 1 \quad (58)$$

and

$$\frac{\partial \lambda_-^L}{\partial \omega^2} = \frac{M_0^4}{k_{\parallel}^2 (M_0^2 - M_1^2) + M_0^4} \quad (59)$$

Again, the ghost content of the theory may change only at $M_0^2 = 0$ (but does not change at this point) or when $M_0^2 - M_1^2 < 0$. The second condition is different for the Lorentz and Euclidean eigenvalues, while the first one is the same. Moreover, the value of $\frac{\partial \lambda}{\partial \omega^2}$ is the same in both cases provided $M_1 = 0$ (the counterpart of $m_1 = 0$ condition in the gravity theory).

DVZ-jump: The derivatives $\frac{\partial \lambda}{\partial k_{\parallel}^2}$ on mass shell are now

$$\frac{\partial \lambda_i^L}{\partial k_{\parallel}^2} = -1 \quad (60)$$

and

$$\frac{\partial \lambda_{\pm}}{\partial k_{\parallel}^2} = \begin{pmatrix} 0 \\ 1 \end{pmatrix} \quad (61)$$

Therefore, again both at $M_0 = 0$ and $M_1 = 0$ there is the DVZ jump.

Now, the lesson is that the Lorentz and Euclidean eigenvalues give the same dispersion laws and, therefore, the same superluminal and tachyon conditions. Moreover, at least, at the case under consideration they give rise to the same DVZ-jump condition. The only difference is in the ghost content conditions. However, even these latter are same provided $M_1 = 0$ in the vector theory case, or $m_1 = 0$ in the gravity case.

Note that the Lorentz eigenvalues are often simpler to use, especially in the Lorentz-invariant theories ($M_0 = M_1$ in formulas above). Indeed, in the latter case the eigenvalues becomes functions of only the combination $-\omega^2 + k_{\parallel}^2$ and can be calculated at the rest frame (where $k_{\parallel} = 0$). This simplifies calculations much, and if the ultimate results coincide, one would prefer to use exactly the Lorentz eigenvalues.

Appendix II. Ghosts and tachyons

In this appendix we very briefly comment on the terminology, used in s.5 of the main text.

Ghosts. A typical example of ghost emerges in the theory of a vector field with the Lagrangian

$$-(\partial_\mu A_\nu)^2 = -\dot{A}_0^2 + \dot{\vec{A}}^2 - \vec{k}^2(A_0^2 - \vec{A}^2) \quad (62)$$

Clearly, A_0 has a "wrong" sign in front of the kinetic term and thus energy is unbounded from below. This means that there can be problems in constructing a full set of normalized states, or – if the theory is adequately modified at the strong-field regime – with making the answers independent of this kind of modification. Such problems are typical for ghosts and one can naturally wish to see when they can arise. At the same time, there is nothing bad seen in the *spectrum* of the theory, if we define it with the help of the Lorenz-invariant metric I_L : $(\partial_{\mu\nu}^2 - \lambda\eta_{\mu\nu})A^\nu = 0$ provides the same spectrum $\lambda = -\omega^2 + \vec{k}^2$ for all components A^ν . If one wants to trace this type of ghosts already at the level of spectral study, one should better use Euclidean eigenvalues with $\eta_{\mu\nu}$ substituted by $\delta_{\mu\nu}$, as suggested in [14].

However, example (62), though standard, is not fully representative. Ghost appears here due to the vector nature of the field A_μ , but this does not mean that *all* ghosts should emerge for *this* reason only. However, if the *raison-d'être* is different, switching from Lorentzian to Euclidean eigenvalues does not help, as we also saw in [14] in analysis of the scalar ghosts. Actually, what matters in a complicated theory is not a particular criterium used to identify ghosts, what matters is how normal particles turn into ghosts and/or back to normal as one moves around in the moduli space \mathcal{M} , and to see this many different criteria can be used. In s.5 we mentioned the simple criterium (12), where in the case of scalars one can use both Lorentzian and Euclidean eigenvalues, as we do in the present paper and in [14] respectively, so that one can compare the results. As well as we can judge, criterium (12) is also in accord with [3].

Though this has no direct relation to content of the present paper, in this Appendix we also remind briefly what is bad (or good) about ghosts and tachyons. Usually one is afraid of ghosts for the three reasons:

- (i) they can grow in time,
- (ii) they can have negative norms and thus violate perturbative unitarity,
- (iii) they interact badly with normal particles.

Actually, these reasons seem different and not obligatory related to each other.

The first reason (i) is pure classical: if one begins with the Lagrangian $\alpha\dot{\phi}^2 - V(\phi)$ with a positive potential ϕ and then change the sign of α from positive to negative, then one immediately and in accordance with criterium (12) obtains solutions with imaginary frequencies, which either grow or decrease in time, instead of oscillating.

It deserves noting that within the standard framework of QFT perturbation theory one deals only with *decreasing* or oscillating solutions. Indeed, if one has a free relativistic particle with the action

$$\int \left(-\omega^2 + \varepsilon^2(\vec{k}) \right) |\phi(\vec{k})|^2 d\omega d\vec{k} \quad (63)$$

one got used to define the Feynman ("casual") propagator as follows:

$$\int \frac{e^{i\omega t} d\omega}{\omega^2 - \varepsilon^2(\vec{k}) - i0} = \frac{1}{2\varepsilon(\vec{k})} \int \left(\frac{1}{\omega - \varepsilon(\vec{k}) - i0} - \frac{1}{\omega + \varepsilon(\vec{k}) + i0} \right) e^{i\omega t} d\omega = \frac{\theta(t)e^{i\varepsilon(\vec{k})t} + \theta(-t)e^{-i\varepsilon(\vec{k})t}}{2\varepsilon(\vec{k})} \quad (64)$$

which is interpreted as a particle with the dispersion rule $\omega = +\varepsilon(\vec{k}) > 0$ propagating forward in time and antiparticle with $\omega = -\varepsilon(\vec{k}) < 0$ propagating backwards in time. Technically, the integration contour is closed by adding an infinitely remote semicircle in the upper half-plane (with $\text{Im } \omega > 0$) for $t > 0$ and in the lower half-plane (with $\text{Im } \omega < 0$) for $t < 0$. Accordingly contributing are different items, with poles lying in the upper and lower half-planes respectively. This very fact implies that the propagator *can not* grow with time at $t > 0$ and *can not* grow backwards in time at $t < 0$: exponents are never positive. One should also take into account different orientations of closed contour in two cases, and factor $2\pi i$ is included into the definition of integral.

If we now consider a more general action

$$\int \left(-f(\vec{k})\omega^2 + g(\vec{k}) \right) |\phi(\vec{k})|^2 d\omega d\vec{k} \quad (65)$$

where $f(\vec{k})$ and $g(\vec{k})$ can become negative at some values of \vec{k} (see Fig.5), then the same propagator becomes more involved, but exponential growth does never occur:

$$\int \frac{e^{i\omega t} d\omega}{f(\vec{k})\omega^2 - g(\vec{k}) - i0} = \begin{cases} \frac{\theta(t)e^{it\sqrt{g/f(\vec{k})}} + \theta(-t)e^{-it\sqrt{g/f(\vec{k})}}}{2\sqrt{fg(\vec{k})}} & \text{when } \begin{matrix} f(\vec{k}) > 0 \\ g(\vec{k}) > 0 \end{matrix} \\ -\frac{\theta(t)e^{-t\sqrt{|g/f(\vec{k})|}} + \theta(-t)e^{t\sqrt{|g/f(\vec{k})|}}}{2\sqrt{|fg(\vec{k})|}} & \text{when } \begin{matrix} f(\vec{k}) < 0 \\ g(\vec{k}) > 0 \end{matrix} \\ \frac{\theta(t)e^{-t\sqrt{|g/f(\vec{k})|}} + \theta(-t)e^{-t\sqrt{|g/f(\vec{k})|}}}{2\sqrt{|fg(\vec{k})|}} & \text{when } \begin{matrix} f(\vec{k}) > 0 \\ g(\vec{k}) < 0 \end{matrix} \\ \frac{\theta(t)e^{-it\sqrt{g/f(\vec{k})}} + \theta(-t)e^{it\sqrt{g/f(\vec{k})}}}{2\sqrt{fg(\vec{k})}} & \text{when } \begin{matrix} f(\vec{k}) < 0 \\ g(\vec{k}) < 0 \end{matrix} \end{cases} \quad (66)$$

Thus, we see that the choice of retarded and advanced Green functions is defined by the *relative signs* in front of different components of kinetic terms *with respect to* auxiliary term $i\epsilon|\phi(\vec{k})|^2$, added to the action. Hence, this choice depends on the definition of the norm for the field. In this paper we assume that these norms are defined by Minkowski metric $\eta_{\mu\nu}$, namely for the gravity field $\|h\|^2 = h_{\mu\nu}h_{\alpha\beta}\eta^{\mu\alpha}\eta^{\nu\beta} = h_{\mu\nu}h^{\mu\nu}$. In [14] we used instead a Euclidean norm $\|h\|_E^2 = \sum_{\mu,\nu=0}^{d-1} h_{\mu\nu}^2$. The disadvantage of Lorentzian norm is that by using it we allow existence of fields with negative norms "by hands", what does not happen with the Euclidean choice, which therefore can be better for analysis of the physical properties of the theory *per se* – as we claimed in [14] – already for this simple reason. However, in Lorentz-invariant theories (like that of gauge-violating massive vectors) the Lorentzian choice looks more "natural" (preserving Lorentz invariance), while Lorentz-violation is introduced as a *deformation* of Lorentz-invariant model and thus does not allow an abrupt switch from Lorentzian to Euclidean norm. Since in this paper we are more concentrated on formal approaches to the study of eigenvalue "bundle" over the moduli space of theories than on the physical properties of massive gravity, we perform all analysis in terms of Lorentzian norms and eigenvalues. For analysis of Euclidean norms and eigenvalues – which we think is more physically justified – see [14].

Another typical example of the problem (ii) is well familiar from conformal field theory: Virasoro descendants of some "good" states can easily happen to possess negative norms (and one tries to get rid of them in construction of "unitary" CFT models). In fact here, like in the previous example of negative norms for the zero-component of a vector field, the problem arises only when one imposes a symmetry requirement on the metric in the space of fields. In CFT example one requires that the Virasoro operators are Hermitian w.r.t. the scalar product, induced by the norm. However, when symmetries are explicitly violated, already at the classical level – that of the Lagrangian – there is no need to impose any type of symmetry requirements on the norms and measures (which define quantization rules), one can always use positively definite norms on entire field space, and in the limit where symmetries are restored and ghosts decouple the two procedures – with invariant and non-invariant norms – are actually equivalent, though sometime it can be somewhat tedious to demonstrate. Thus it is not so simple to decide what really happens, either unitarity is broken by existence of negative-norm states or, more probably, an *anomaly* occurs: the symmetry and excitation spectrum of emerging theory is different from the one that one could naively expect.

The really serious problem can be the third one, (iii). The simplest example is again that of A_0 -component of the vector field. In order to have all norms positive in this theory one needs to define vacuum state as annihilated by *annihilation* operators $\hat{a}_i|0\rangle = 0$ for all the spatial components \vec{A} of the vector field, and by *creation* operator $\hat{a}_0|0\rangle = 0$ for A_0 . This means that one actually loses a possibility to define a Lorentz-invariant vacuum. This could still be tolerated, but the situation becomes dramatically worse when one tries to switch on interactions. To the best of our knowledge so far no consistent *perturbation* theory was developed for interacting ghosts and normal particles (though one can easily believe that there are problem-free non-perturbative theories of this kind: say when globally energy is positively defined while one begins with a perturbation theory around a local maximum).

Tachyons. This term is unfortunately used in total contradiction with its literal meaning. Lexically, "tachyon" referred to superluminal propagation, but today we have to use the word "superluminal" for such particles, because "tachyon" is used to mean something else. Actually, tachyon occurs when vacuum is perturbatively unstable, then it can start to decay independently at casually-disconnected points and this can *look like* a propagation of a superluminal excitation, but physically the reason is obvious and very different from real superluminals. From the spectral point of view, what is now called tachyon is the pole in the propagator,

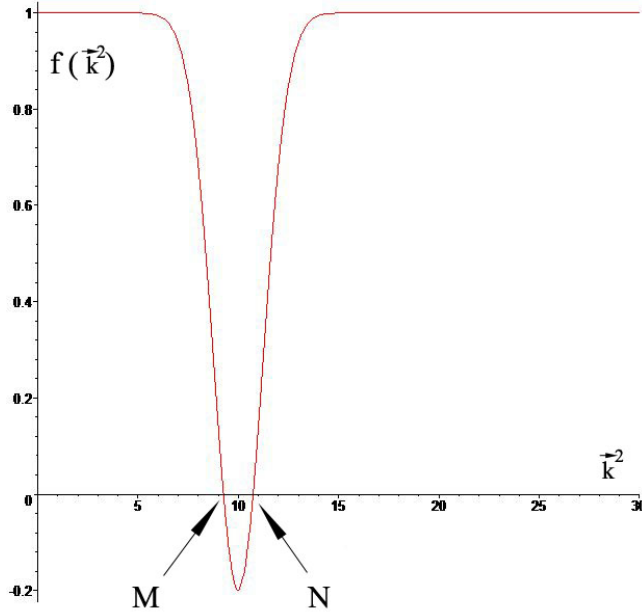


Figure 5: A typical example of function $f(\vec{k}^2)$ in Lorentz-violating dispersion relation $\lambda = -f(\vec{k}^2)\omega^2 + \vec{k}^2 + m^2 = 0$. For most values of space momenta we have just an ordinary relativistic particle, while in some region in \vec{k} space it becomes superluminal, then carries an *instantaneous* interaction (just like Newton-Coulomb-Yukawa potential) – this happens at points M and N – and between M and N it behaves like ghost, i.e. describes advanced rather than retarded interaction.

occurring at vanishing frequency $\omega = 0$. The archetypical example is the case $f(\vec{k}) = 1$, $g(\vec{k}) = \vec{k}^2 - m^2$ with the "wrong" sign in front of the mass term. Then, at small t

$$\int \frac{e^{-i\vec{k}\vec{x}} d^3k d\omega}{\omega^2 - k^2 + m^2 - i0} \sim \frac{m^2}{r} [J_1(mr) + N'_0(mr)] \quad (67)$$

where J_k and N_k are the Bessel and Neumann cylindric functions correspondingly, and the prime means the derivative w.r.t. the argument. Therefore, in this case the propagator behaves as e^{imr}/r at large distances (small \vec{k} , there is no pole), and is singular, $1/r$ at small distances (large \vec{k} , there is a pole). The indication of a tachyon is non-decaying correlation at infinity. Note that simultaneously at large distances the time correlation exponentially decays and at small distance does not. This means that at large distances the time and spatial coordinates interchanged, and the causality is violated (correlations do not fall outside the light cone).

Appendix III. Analysis of a model characteristic equation

In order to illustrate the eigenvalue behavior it is instructive to examine a model characteristic equation which is quadratic but not quartic in λ :

$$C(\lambda) = \lambda^2 + (2k^2 + \alpha)\lambda + (\beta k^2 + \gamma) = 0 \quad (68)$$

In this case, one can explicitly solve all equations, and we use this to illustrate the way the information can be extracted from plots (which are equally available beyond the quadratic case). The two eigenvalues are

$$\lambda_{\pm} = \frac{-(2k^2 + \alpha) \pm \sqrt{D}}{2}, \quad D = (2k^2 + \alpha)^2 - 4(\beta k^2 + \gamma) = (2k^2 + \alpha - \beta)^2 + (2\alpha\beta - \beta^2 - 4\gamma) \quad (69)$$

Their k^2 -derivatives are equal to

$$\frac{\partial \lambda_{\pm}}{\partial k^2} = -1 \pm \frac{2k^2 + \alpha - \beta}{\sqrt{D}}, \quad (70)$$

so that

$$\frac{\partial \lambda_+}{\partial k^2} \cdot \frac{\partial \lambda_-}{\partial k^2} = \frac{D - (2k^2 + \alpha - \beta)^2}{D} = \frac{(2\alpha\beta - \beta^2 - 4\gamma)}{D} \quad (71)$$

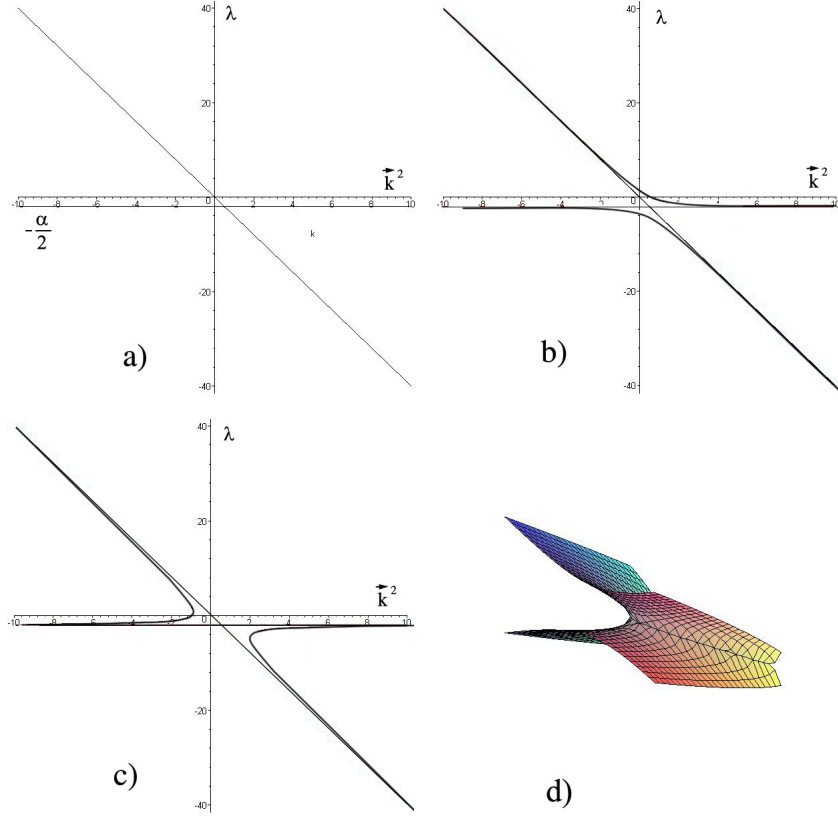


Figure 6: Eigenvalues (69) as functions of k^2 at different values of parameters α , β and γ . **a)**. The case when $2\alpha\beta - \beta^2 - 4\gamma = 0$, discriminant D is a full square and λ_{\pm} become linear functions of k^2 , or $\lambda_{\pm} = \frac{-(2k^2 + \alpha) \pm |2k^2 + \alpha - \beta|}{2}$, to be exact. The horizontal line is at $\lambda_{\infty} = -\frac{1}{2}\beta$. **b)**. Resolution of the crossing singularity at $2\alpha\beta - \beta^2 - 4\gamma > 0$, when λ_{\pm} are real at all values of k^2 . Asymptotically at $k^2 \rightarrow \pm\infty$ eigenvalues tend to $\lambda_{\infty} = -\lim_{k^2 \rightarrow \infty} \frac{\beta k^2 + \gamma}{2k^2 + \alpha} = -\frac{1}{2}\beta$ (or to infinity). Punctured lines show the same cross as in Fig.a, the role of the resolution (deformation) parameter is played by γ . **c)**. Resolution of the crossing singularity at $2\alpha\beta - \beta^2 - 4\gamma > 0$, when λ_{\pm} fail to be real-valued at some k^2 . **d)**. The 3d plot of λ_{\pm} as function of k^2 and γ . The saddle structure is clearly seen. It degenerates to Fig.2a in the special case of (75) when $2\alpha\beta - \beta^2 - 4\gamma = 4(d-1)B^2$ and is never negative.

while the resultant in the numerator of (20) is

$$\text{resultant}_{\lambda} \left(C(\lambda), \frac{\partial C(\lambda)}{\partial k^2} \right) = \det \begin{pmatrix} 1 & 2k^2 + \alpha & \beta k^2 + \gamma \\ 2 & \beta & 0 \\ 0 & 2 & \beta \end{pmatrix} = -(2\alpha\beta - \beta^2 - 4\gamma) \quad (72)$$

Denominator of (20) is simply D .

This implies that $\frac{\partial \lambda}{\partial k^2} = 0$ in two cases: either when $k^2 = \pm\infty$ and discriminant $|D| = \infty$ or when $2\alpha\beta - \beta^2 - 4\gamma = 0$ and D is a full square, so that λ_{\pm} become linear functions of k^2 . This property is nicely illustrated by the plots in Fig.6. In this way one can extract information from eq.(20) and from plots, what is especially useful in the realistic case (32), when $C_4(\lambda)$ has degree 4 and analytical approach is less straightforward.

Explicitly in the linearized Lorentz-violating gravity (1) the characteristic polynomial for the scalar modes is equal to

$$\begin{aligned} C_4(\lambda) = & \lambda^4 + \left((d-3)(-\omega^2 + \vec{k}^2) + m_0^2 - m_1^2 - 2m_2^2 + (d-1)m_3^2 \right) \lambda^3 + \\ & + \left(-(d-2)(-\omega^2 + \vec{k}^2)^2 - ((d-3)(m_0^2 - m_1^2 - m_2^2) - (d-1)m_3^2)\omega^2 + ((d-3)(m_0^2 - m_1^2 - m_2^2 + m_3^2) - 2(d-2)m_4^2)\vec{k}^2 - \right. \\ & \left. - m_0^2 m_1^2 - 2m_0^2 m_2^2 + 2m_1^2 m_2^2 + m_2^4 + (d-1)(m_0^2 m_3^2 - m_1^2 m_3^2 - m_2^2 m_3^2 - m_4^4) \right) \lambda^2 - \\ & - \left((d-2) \left[(m_0^2 - m_1^2)\omega^4 - 2(m_0^2 - m_2^2 + m_3^2 - m_4^2)\omega^2 \vec{k}^2 - (m_1^2 + m_2^2 - m_3^2)\vec{k}^4 \right] - \right. \\ & \left. - ((d-3)(m_0^2 m_1^2 + m_0^2 m_2^2 - m_1^2 m_2^2) + (d-1)(m_0^2 m_3^2 - m_1^2 m_3^2 - m_4^4))\omega^2 + \right. \\ & \left. + ((d-3)(m_0^2 m_1^2 + m_0^2 m_2^2 - m_0^2 m_3^2 - m_1^2 m_2^2 + m_1^2 m_3^2 + m_4^4) - 2(d-2)(m_1^2 + m_2^2)m_4^2 \right) \vec{k}^2 - \end{aligned} \quad (73)$$

$$\begin{aligned}
& -2m_0^2m_1^2m_2^2 - m_0^2m_2^4 + m_1^2m_2^4 + (d-1)(m_1^2 + m_2^2)(m_0^2m_3^2 - m_4^4) - (d-1)m_1^2m_2^2m_3^2 \lambda + \\
& + \left((d-2) [m_0^2m_1^2\omega^4 - 2(m_0^2m_2^2 - m_0^2m_3^2 - m_1^2m_4^2 + m_4^4)\omega^2\vec{k}^2 - m_1^2(m_2^2 - m_3^2)\vec{k}^4] - \right. \\
& \left. - m_1^2((d-3)m_0^2m_2^2 + (d-1)(m_0^2m_3^2 - m_4^4))\omega^2 + m_1^2((d-3)(m_0^2m_2^2 - m_0^2m_3^2 + m_4^4) - 2(d-2)m_2^2m_4^2)\vec{k}^2 - \right. \\
& \left. - m_0^2m_1^2m_2^4 + (d-1)m_1^2m_2^2(m_0^2m_3^2 - m_4^4) \right)
\end{aligned}$$

At $\vec{k} = 0$, i.e. in the rest frame, the characteristic polynomial (73) factorizes:

$$\begin{aligned}
& C_4(\lambda)|_{\vec{k}=0} = (\lambda + \omega^2 - m_2^2)(\lambda - m_1^2) \cdot \\
& \cdot \left\{ \lambda^2 + \lambda \left(m_0^2 - m_2^2 + (d-1)m_3^2 - (d-2)\omega^2 \right) - m_0^2 \left(m_2^2 + (d-2)\omega^2 \right) + (d-1)(m_0^2m_3^2 - m_4^4) \right\} \quad (74)
\end{aligned}$$

For (2) the last bracket turns into

$$C_2(\lambda) = \lambda^2 + \lambda \left(dB - 2A - (d-2)\omega^2 \right) + \left((d-2)(A-B)\omega^2 + A(A-dB) \right) \quad (75)$$

with the two roots given by the last row in (29),

$$\lambda_{\pm} = A - \frac{dB - (d-2)\omega^2 \pm \sqrt{(d-2)^2(B-\omega^2)^2 + 4(d-1)B^2}}{2} \quad (76)$$

Example (68) can be now used upon identification $k^2 = -\frac{d-2}{2}\omega^2$, $\alpha = dB - 2A$, $\beta = 2(B-A)$, $\gamma = A(A-dB)$ and $2\alpha\beta - \beta^2 - 4\gamma = 4(d-1)B^2 \geq 0$. In general in the rest frame one gets from the last bracket in (74): $\alpha = m_0^2 - m_2^2 + (d-1)m_3^2$, $\beta = 2m_0^2$, $\gamma = (d-1)(m_0^2m_3^2 - m_4^4) - m_0^2m_2^2$ and $2\alpha\beta - \beta^2 - 4\gamma = 4(d-1)m_4^4 \geq 0$. This implies that the singularity is resolved at $\omega^2 = 0$ in the single possible way, which explains the universal structure of Fig.1b.

If instead of $\vec{k} = 0$ we put $\omega = 0$, characteristic polynomial $C_4(\lambda)$ factorizes in a less radical way:

$$\begin{aligned}
& C_4(\lambda)|_{\omega=0} = (\lambda - m_1^2) \left\{ \lambda^3 + \left((d-3)\vec{k}^2 + m_0^2 - 2m_2^2 + (d-1)m_3^2 \right) \lambda^2 + \right. \\
& + \left(- (d-2)\vec{k}^4 + [(d-3)(m_0^2 - m_2^2 + m_3^2) - 2(d-2)m_4^2]\vec{k}^2 + [m_2^4 - 2m_0^2m_2^2 + (d-1)(m_0^2m_3^2 - m_2^2m_3^2 - m_4^4)] \right) \lambda + \\
& \left. + \left((d-2)(m_2^2 - m_3^2)\vec{k}^4 + [(d-3)m_0^2(m_3^2 - m_2^2) + 2(d-2)m_2^2m_4^2 - (d-3)m_4^4]\vec{k}^2 + [m_0^2m_2^4 - (d-1)m_0^2m_2^2m_3^2 + (d-1)m_2^2m_4^4] \right) \right\} \quad (77)
\end{aligned}$$

The roots of this equation are plotted in Fig.4. Of course, in the Lorentz-invariant case (2) this (77) further reduces to $(\lambda - \vec{k}^2 - A)$ times (75), with $-\omega^2$ substituted by \vec{k}^2 .

For the full $C_4(\lambda)$ in (73) the resultants of $C_4(\lambda)$ with $\frac{\partial C_4(\lambda)}{\partial \omega^2}$ and $\frac{\partial C_4(\lambda)}{\partial \vec{k}^2}$ in the numerator of (20) are rather complicated and essentially different, however, they contain two common d -independent factors:

$$\left((m_0^2 + m_1^2)(m_1^2 - m_2^2 + m_3^2) - m_4^4 \right) \quad (78)$$

and

$$\begin{aligned}
& \left(m_4^2\omega^4 - (m_0^2 + m_2^2 - m_3^2)\omega^2\vec{k}^2 - m_4^2\vec{k}^4 - (m_0^2m_4^2 + m_2^2m_4^2 + m_3^2m_4^2)\omega^2 + \right. \\
& \left. + (m_0^2m_3^2 + m_2^2m_3^2 - m_3^4 - 2m_4^4)\vec{k}^2 + (m_0^2m_3^2m_4^2 + m_2^2m_3^2m_4^2 - m_4^6) \right) \quad (79)
\end{aligned}$$

The first factor (78) vanishes in the Lorentz invariant case (2), when one of the eigenvalue lines is obligatory horizontal. Furthermore, $\text{resultant}_{\lambda} \left(C_4(\lambda), \frac{\partial C_4(\lambda)}{\partial \omega^2} \right) \sim \vec{k}^2$, while $\text{resultant}_{\lambda} \left(C_4(\lambda), \frac{\partial C_4(\lambda)}{\partial \vec{k}^2} \right) \sim \omega^2$, so that they vanish at $\vec{k} = 0$ and $\omega = 0$ respectively – in accordance with Figs.1b and 2b, which both contain one horizontal eigenvalue line (associated with the spatial Stueckelberg scalar). In addition, in the rest frame, at $\vec{k} = 0$, the second factor (79) is proportional to m_4 , what corresponds to appearance of the second horizontal eigenvalue line in Fig.1a at $m_4 = 0$. As to the first factor (78), when it vanishes beyond the Lorentz-invariant case (2), it still signals that a horizontal line occurs. In fact, this is the line $\lambda = m_1^2$: if (78) vanishes, then $C_4(\lambda)$ is divisible by $(\lambda - m_1^2)$ for all values of ω and \vec{k} .

Appendix IV. Eigenvalue bundle over the moduli space

1 Deformation of four crosses

The four-cross pattern, Fig.1a, describes the dependence of four scalar eigenvalues of $-\omega^2$ when $m_4^2 = 0$ and $\vec{k}^2 = 0$. Then the two horizontal lines are $\lambda_{sS} = -m_0^2$ and $\lambda_S = m_1^2$, while two other lines with slopes $+1$ (normal particle) and $-(d-2)$ (ghost) are given by $\lambda_{sT} = -\omega^2 + m_2^2$ and $\lambda_{stT} = (d-2)\omega^2 + m_2^2 - (d-1)m_3^2$, i.e. they intersect the ordinate axis at m_2^2 and $m_2^2 - (d-1)m_3^2$ respectively. There are two propagating (on-shell) modes with $\lambda = 0$, one is normal, another one is ghost.

When $m_4^2 \neq 0$ is switched on, Fig.1b, one of the four crossings is resolved: the one between λ_{sS} and λ_{stT} . The intersecting eigenvalues repulse but intersection with the abscissa axis corresponds to a ghost in both cases, $m_0^2 > 0$ and $m_0^2 < 0$: depending on the sign of m_0^2 the on-shell ghost comes from either lower or upper of the two branches. The only exception is the case of $m_0^2 = 0$: then this on-shell mode simply disappears at infinity and the ghost is eliminated, at least at $\vec{k}^2 = 0$.

Switching on $\vec{k}^2 \neq 0$ resolves all the four crossings (even if $m_4^2 = 0$). This adds one more option: that ghost can be eliminated not only when $m_0^2 = 0$ but also when $m_1^2 = 0$, exactly in the same way as above. However, with increasing \vec{k}^2 and m_4^2 the patterns deviate pretty far from the four-crosses of Fig.1a, see Fig.7,8 for some examples. This means that even if ghosts are eliminated in the vicinity of four-cross pattern, they can re-appear at larger values of the momentum \vec{k}^2 . Also the case of large m_4^2 requires more careful analysis.

As clear from Figs.7,8, the only two possibilities to have ghost-free models arise at either $m_0^2 = 0$ or at $m_1^2 = 0$.

2 Analysis through the chain of bifurcations

Analysis of the properties of propagating particles can be performed in a certain order, because actually there is a hierarchy of interesting properties.

1) Plot $\lambda(-\omega^2)$ at fixed \vec{k}^2 and masses or $\lambda(\vec{k}^2)$ at fixed ω^2 and masses. Of interest are on-shell states $\lambda = 0$ and the slopes $-\frac{\partial \lambda}{\partial \omega^2} \Big|_{\lambda=0}$ or $\frac{\partial \lambda}{\partial \vec{k}^2} \Big|_{\lambda=0}$ at these points. In what follows we consider mostly the first option: $\lambda(-\omega^2)$.

2) The signs of derivatives are actually controlled by topology of the graph $\lambda(\omega^2)$, especially by positions of the branching points: zeroes of discriminant $\text{discrim}(C(\lambda))$ where different branches merge or intersect. These critical points ω_{cr}^2 are themselves *not* on-shell, but they actually define the properties of on-shell modes. They depend both on \vec{k}^2 and masses. Of primary interest is their dependence on space momentum \vec{k}^2 at fixed masses.

3) The properties of on-shell particles change qualitatively at bifurcation points when ω_{cr}^2 merge, vanish or go to infinity. This is controlled by zeroes of the next-level discriminant $\text{discrim}(\omega_{cr}^2(\vec{k}^2))$. These zeroes \vec{k}_{cr}^2 (masses) depend only on masses and change when the masses change, i.e. when we move along the moduli space \mathcal{M} . At some points of \mathcal{M} there can be regions in momentum space where on-shell particles are ghosts, and regions where they are always normal or are ghosts for all values of \vec{k} .

4) The boundaries between these regions are defined by the next-order discriminants $\text{discrim}(\vec{k}_{cr}^2(masses))$. One can again make an iterative study: change first some of masses, most conveniently, m_4^2 , and then the others, considering higher and higher order discriminants at each step.

3 Examples

We give now examples of such hierarchical analysis.

1) Some plots of the four-branch function $\lambda(-\omega^2)$ are shown in Figs.7 and 8. In Fig.7 the values of masses are fixed and different plots are for different values of \vec{k}^2 . In Fig.8 we fix $\vec{k}^2 = 1$ instead, but change two of the five masses (m_0^2 and m_1^2) instead. If another mass (m_4^2) is changed we get a very different pattern, Fig.9. There is no problem in making many more plots of this kind. The problem is to find some reasonable way to put this huge collection in order. This is what above hierarchical procedure is supposed to do.

2) From Figs.7 and 8 it is clear that the whole pattern is very well controlled by position of the branching points (where the tangent line becomes vertical). These branching points can be defined by pure algebraic means: they are zeroes of discriminant: solutions to the equation

$$\text{discrim}_\lambda(C(\lambda)) = 0 \tag{80}$$

Discriminant at the l.h.s. is a little too long to present here, but it is an explicit polynomial⁶ and can be easily evaluated for any particular set of masses. After that its zeroes can be found numerically and they are plotted in the center of Fig.11 as functions of \vec{k}^2 for the same values of masses that were chosen in Fig.7. One can easily compare Figs.7 and 11, and the moral is that essential information about the pattern in Fig.7 is actually contained in the far simpler and pure algebraic plot in Fig.11. In fact, one can easily plot zeroes of the same discriminant as functions of masses instead of \vec{k}^2 and reproduce the essential properties of Fig.8 instead of Fig.7.

3) Fig.11 itself can be changed if we vary remaining parameters. In Fig.11 positions of the branching points were plotted as functions of \vec{k}^2 . Fig.12 shows what happens with Fig.11 when one of the mass parameters is changed. The difference between Figs.11 and Fig.12 could be systematically controlled in an algebraic way, if we look at zeroes of the *repeated discriminant* – the crossing/merging points of the three branches in Fig.11. This structure is discussed below and pictured in Fig.10-13.

4) Procedure can be repeated again and again, going to higher and higher codimension in the moduli space \mathcal{M} . Thus we obtain a systematic approach to the study of bifurcations/reshufflings of eigenvalue bundle and to construction of phase diagrams of the theory.

4 The bundle structure

It is instructive to present the same in a slightly different words – and pictures, – by making more explicit the structure of *eigenvalue bundle* over the moduli space of linearized massive gravity.

Let us fix the values of four masses, $m_0^2 = 4$, $m_1^2 = 0$, $m_2^2 = 4$, $m_3^2 = 6$ and look what happens when we change m_4^2 from 2.64 to 3.53. The choice of masses is rather arbitrary with two exceptions: m_1^2 is taken vanishing in order to look at appearance and disappearance of the on-shell ghost, and m_4^2 is chosen to vary in the vicinity of the critical value, where

$$\Delta \equiv m_0^2(m_3^2 - m_2^2) - m_4^4 = 0 \quad (81)$$

and where an interesting bifurcation occurs. In this particular case the critical value of m_4^2 is $m_0\sqrt{m_3^2 - m_2^2} = 2\sqrt{2} = 2.828427\dots$

Thus we begin from $m_4^2 = 2.64$. Over this point of the moduli space \mathcal{M} there is a fiber of our "bundle", consisting of the 4-branched function $\lambda(\omega, \vec{k})$. Instead of hanging such 3-dimensional fiber over the base point we do another thing: we hang first a $2d$ plot of $\omega_{crit}^2(\vec{k}^2)$, which shows how the three critical points α, β, γ – the three zeroes of discriminant $\text{discrim}(C(\lambda))$ – change with the variation of momentum \vec{k}^2 . After that over each point of *this* fiber – which we call *discriminant fiber* in what follows – we hang the $2d$ plot $\lambda(-\omega^2)$ (the *eigenvalue fiber*), as shown in Fig.10. In this particular case of $m_4^2 = 2.64$ discriminant fiber consists of a single real branch and only a single branching point α is seen in the eigenvalue plot. We show also the enlarged vicinity of α in accompanying figure, where one non-very-interesting branch is not actually seen. It is clear from this picture that there is a single on-shell scalar, it is located at $\omega^2 = 0$ and it is ghost, because the slope of the branch is negative at the intersection with abscissa axis. In fact, this is a very exotic excitation, being simultaneously a carrier of instantaneous interaction $\omega^2 = 0$ and a ghost since $d\lambda/d\omega^2 < 0$ on shell. Its characteristic dispersion relation is $-\omega^2\vec{k}^2 = i\epsilon$ [14]. Actually it remains of this same kind for all values of m_4^2 , only the coefficient at the l.h.s. becomes a sophisticated function of \vec{k}^2 and can even change sign with the variation of \vec{k}^2 . The physical implications of such "instantaneous" excitation in the spectrum remain an interesting subject for future investigation.

Now we start increasing m_4^2 . At $m_4^2 = 2.828428\dots$, i.e. at the critical value $\Delta = 0$ a new couple of branches shows up in discriminant fiber (they were complex at lower values⁷ of m_4^2) and they get well separated soon enough, we show an example at $m_4^2 = 2.9$. It is seen that at this value of m_4^2 one of the two new branches merges with the old one at $\vec{k}^2 \approx 2$ – and this is reflected in the properties of the eigenvalue fiber.

At larger value of $m_4^2 = 3.53553\dots$ the other two branches merge as well, and it is quite interesting to look at the corresponding collection of the eigenvalue plots, shown enlarged in Fig.11. We see that with the change of \vec{k}^2 the on-shell scalar converts from normal particle at $\vec{k}^2 < 1.623759\dots$ into ghost and then back into normal

⁶As a function of its coefficients discriminant of the order-4 polynomial $C(\lambda) = \sum_{i=0}^4 C_i \lambda^i$ is given by

$$\begin{aligned} & -4C_4C_2^3C_1^2 + 16C_4C_2^4C_0 - 128C_4^2C_0^2C_2^2 - 27C_3^4C_0^2 - 6C_4C_0C_3^2C_1^2 + 144C_4C_0^2C_2C_3^2 + 144C_4^2C_0C_2C_1^2 + 18C_4C_3C_1^3C_2 + C_2^2C_3^2C_1^2 - \\ & -4C_2^3C_3^2C_0 - 4C_3^3C_1^3 + 256C_4^3C_0^3 - 192C_4^2C_0^2C_3C_1 - 80C_4C_3C_1C_2^2C_0 + 18C_3^3C_1C_2C_0 - 27C_4^2C_1^4 \end{aligned}$$

It is a polynomial of degree $2(4-1) = 6$ in the coefficients and can be read from the celebrated Sylvester formula or represented as a combination of two simple diagrams, see [18, 19]. Substitution of coefficients expression through masses, frequency and momentum from (73) makes this expression rather lengthy.

⁷One can see that the two complex branches are already very close to become real by looking at eigenvalue plot at $m_4^2 = 2.64$ and $\vec{k}^2 = 6$: it is pretty clear that something is going to happen, and this behavior of the eigenvalue curves signals that discriminant zero is nearby – just not seen in the real section of generic complex picture.

particle at $\vec{k}^2 > 11.39337\dots$. Note that the *crossing* of branches in discriminant fiber at $\vec{k}^2 \approx 3.85$ does not cause any reshuffling in the eigenvalue fiber: this is because this is *crossing* rather than *merging* of branches.

It deserves mentioning that the slightly-virtual *instantaneon* can actually be described analytically: at small values of ω^2 the corresponding eigenvalue is

$$\lambda_{instant} = \frac{2(d-2)\Delta \cdot \omega^2 \vec{k}^2}{(d-2)(m_3^2 - m_2^2)\vec{k}^4 - [(d-3)\Delta + 2(d-2)m_2^2 m_4^2]\vec{k}^2 + (d-1)m_2^2(m_0^2 m_3^2 - m_4^4) - m_0^2 m_2^4} + O(\omega^4) \quad (82)$$

where Δ is given by (81). One can easily check that this simple formula provides a full description of the bifurcations which we are shown in the above pictures. Thus, the exactly solvable example confirms the results of generally applicable discriminant analysis.

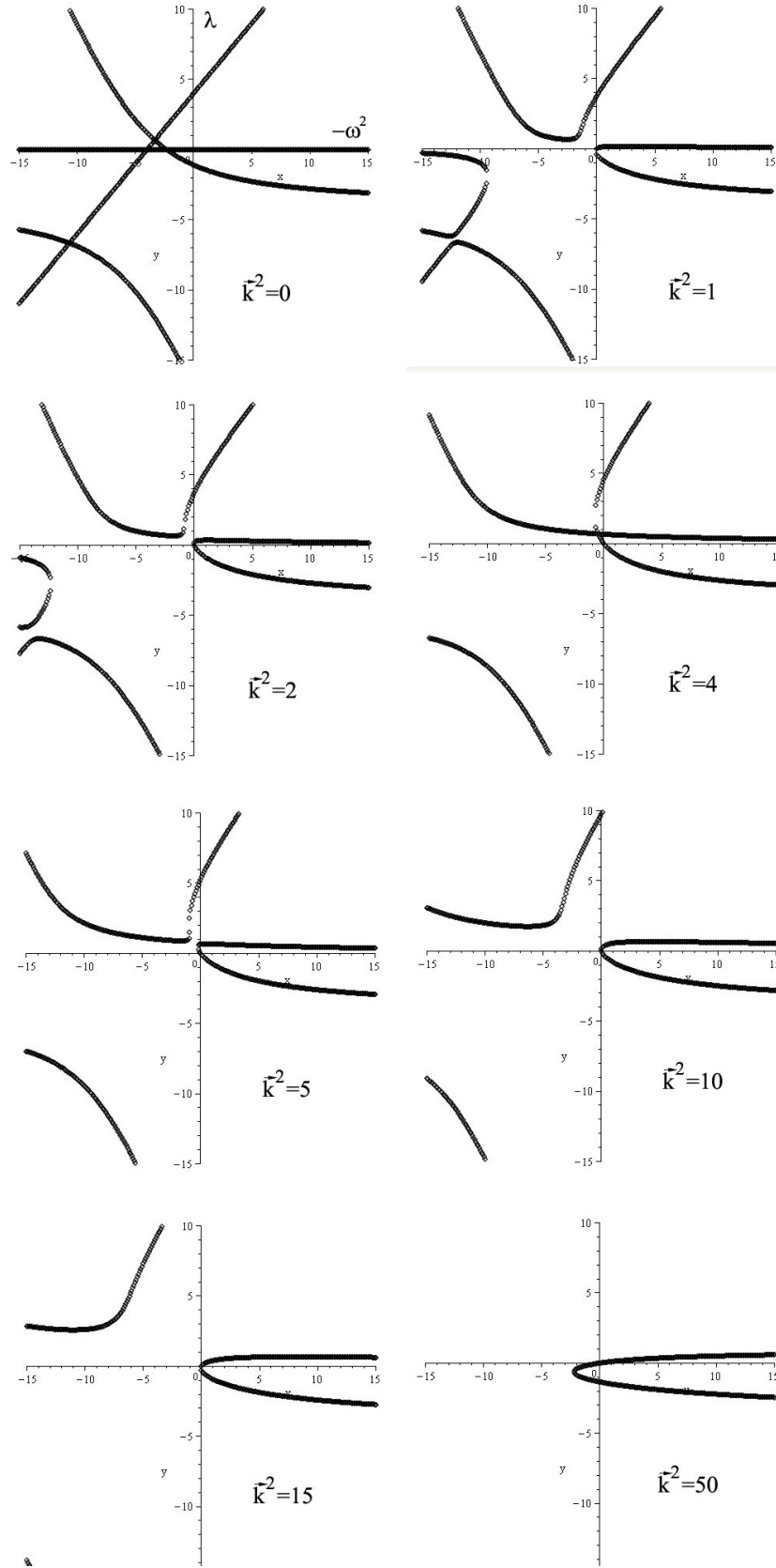


Figure 7: Pattern of eigenvalues dependence on $-\omega^2$ for masses $m_0^2 = 4$, $m_1^2 = 0$, $m_2^2 = 4$, $m_3^2 = 6$, $m_4^2 = 3.53553\dots$ and different \bar{k}^2 . The slope of the curve $\lambda(-\omega^2)$ at $\lambda = 0$ (on shell) changes from positive to negative and back to positive, thus demonstrating existence of a window in \bar{k}^2 space where propagating particle behaves as a ghost – in accordance with Fig.11.

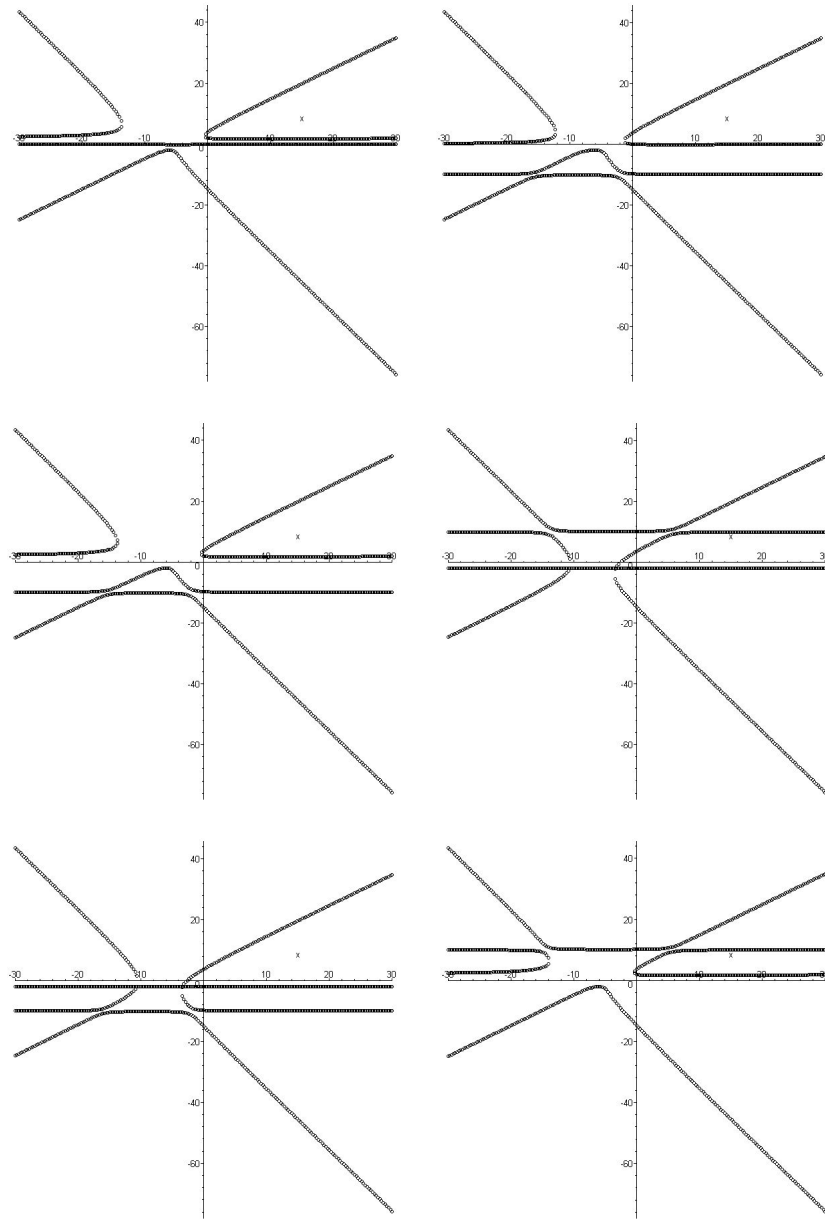


Figure 8: The graph of the dependence of eigenvalues on ω^2 for $k^2 = 1$ and different values of masses m_1 and m_0 . Masses at the left pictures (down from above) are equal to $m_0^2 = 0, m_1^2 = 2, m_2^2 = 4, m_3^2 = 6, m_4^2 = 0$; $m_0^2 = 10, m_1^2 = 2, m_2^2 = 4, m_3^2 = 6, m_4^2 = 0$; $m_0^2 = 10, m_1^2 = -2, m_2^2 = 4, m_3^2 = 6, m_4^2 = 0$. Similarly, those at the right pictures are $m_0^2 = 10, m_1^2 = 0, m_2^2 = 4, m_3^2 = 6, m_4^2 = 0$; $m_0^2 = -10, m_1^2 = -2, m_2^2 = 4, m_3^2 = 6, m_4^2 = 0$; $m_0^2 = -10, m_1^2 = 2, m_2^2 = 4, m_3^2 = 6, m_4^2 = 0$. Therefore, the two upper pictures correspond to the case when one of these masses is equal to zero.

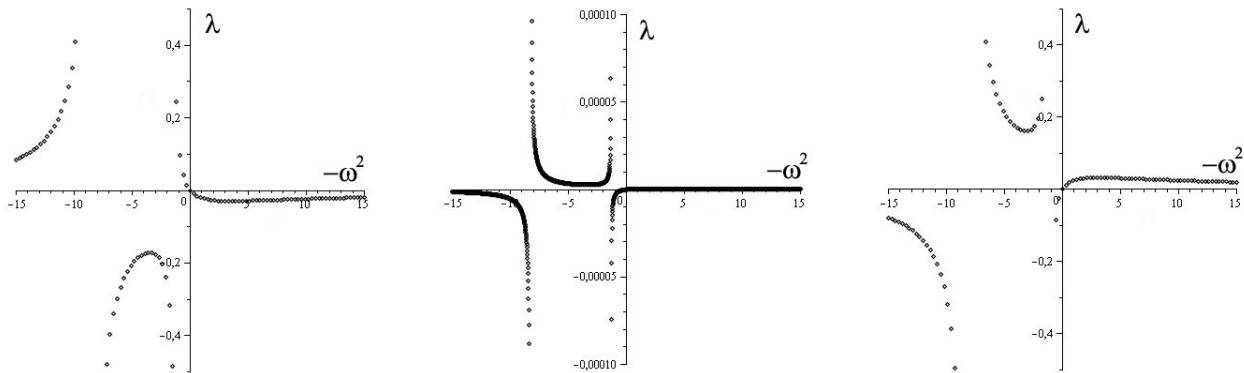


Figure 9: Variation of the eigenvalue curves in Fig.7 with the change of mass m_4 : $m_4^2 = 3; 2.82843; 2.64575$ (from the left to the right). The scale in the middle picture is different.

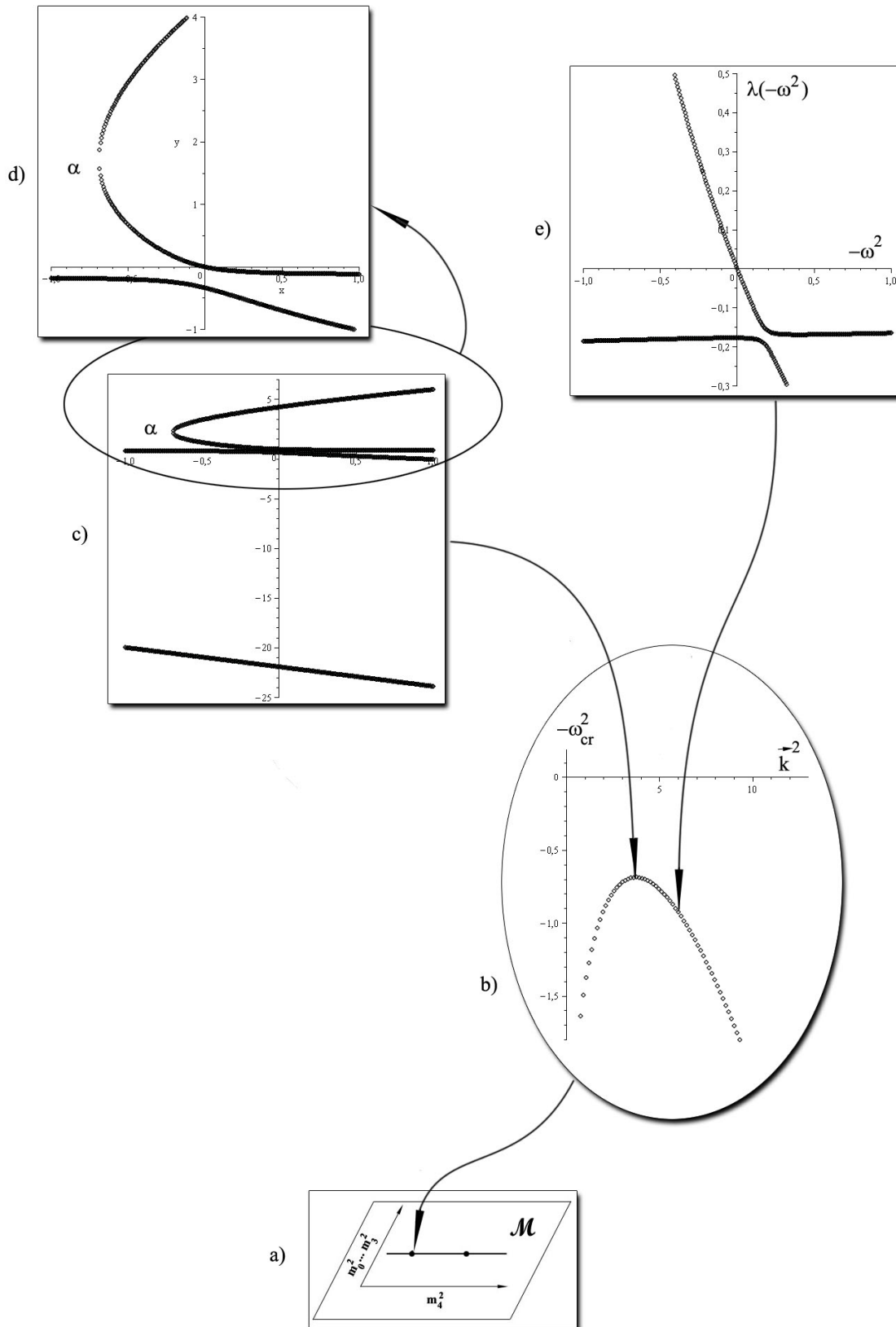


Figure 10:

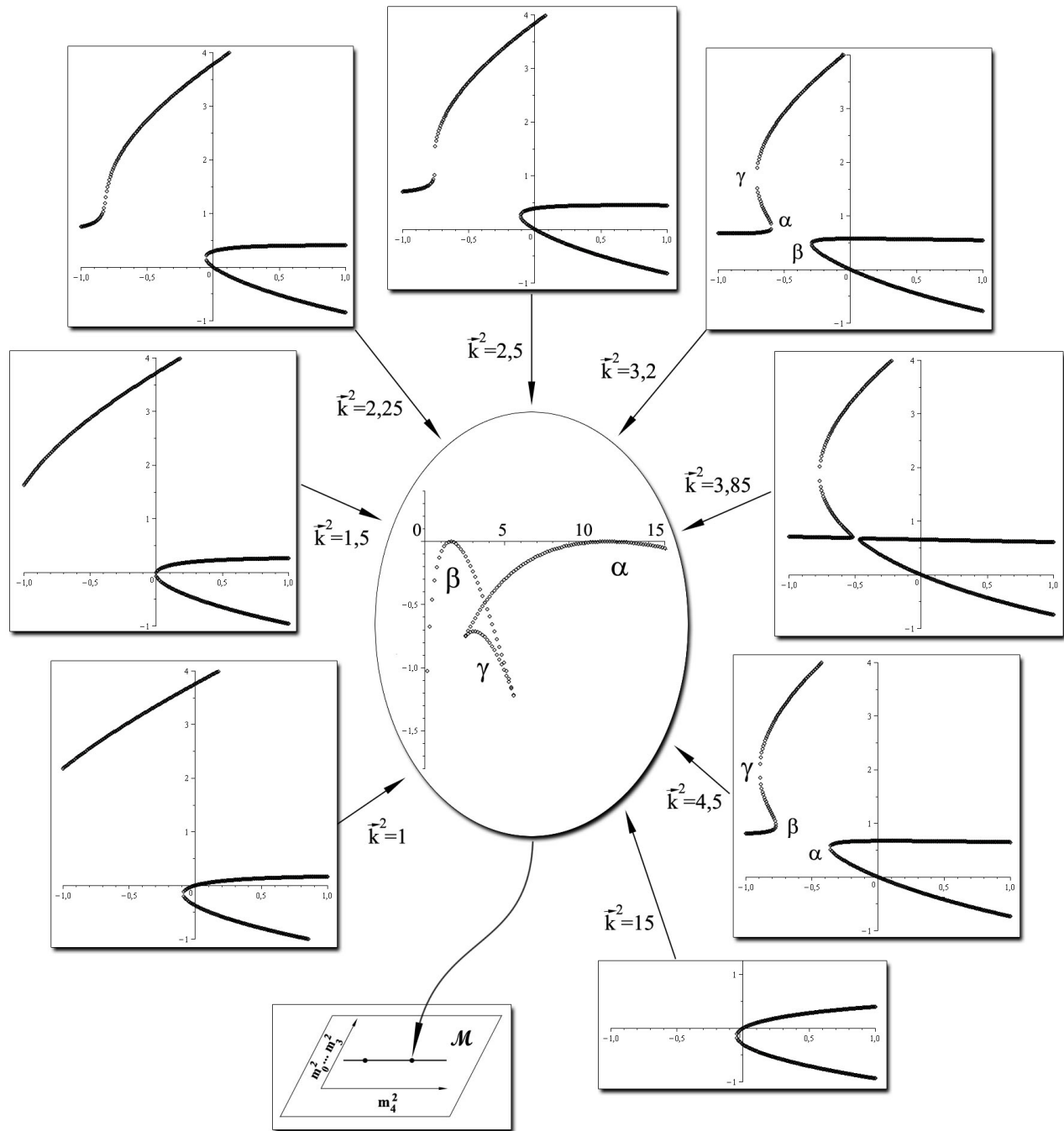


Figure 11:

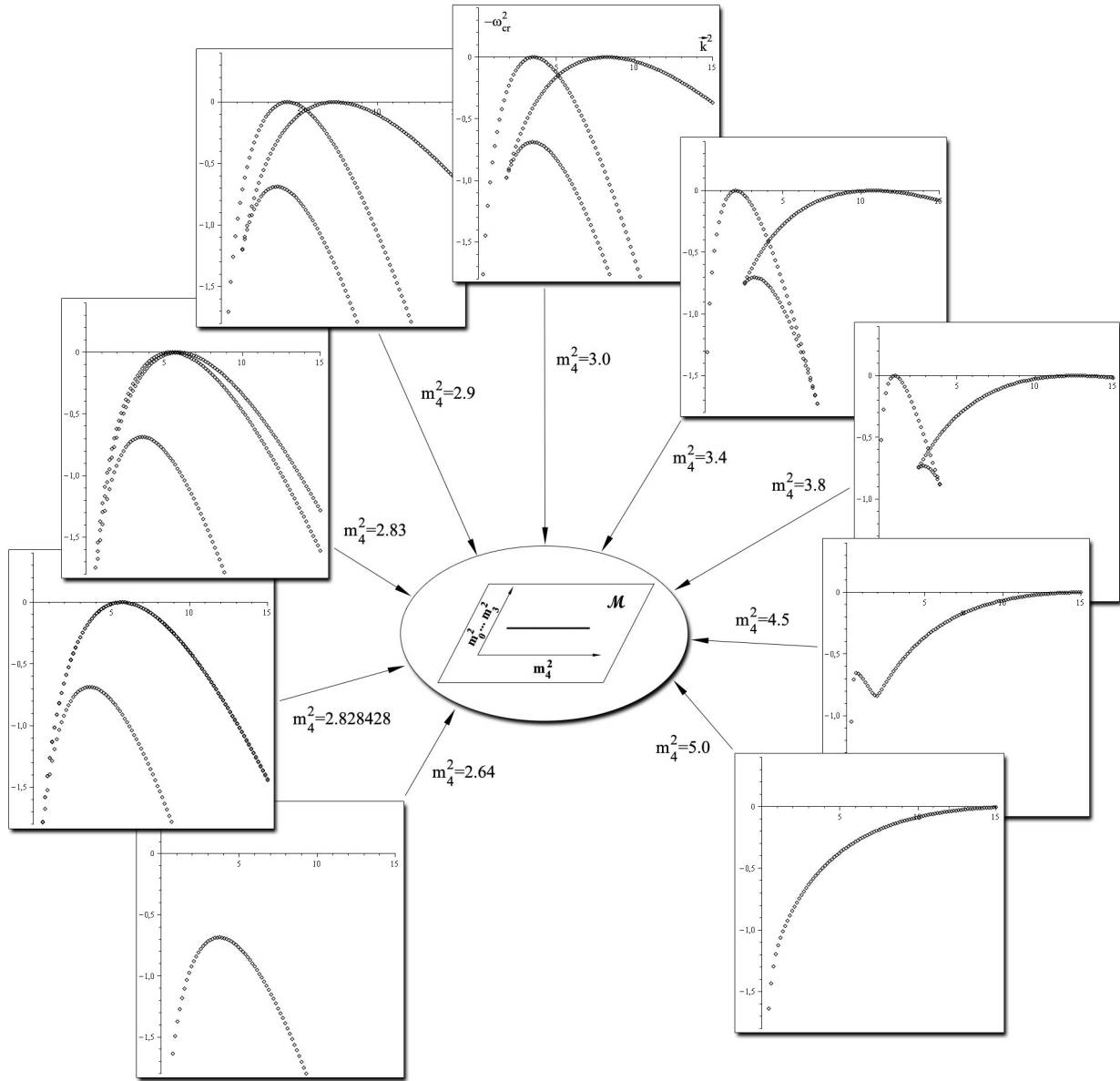


Figure 12:

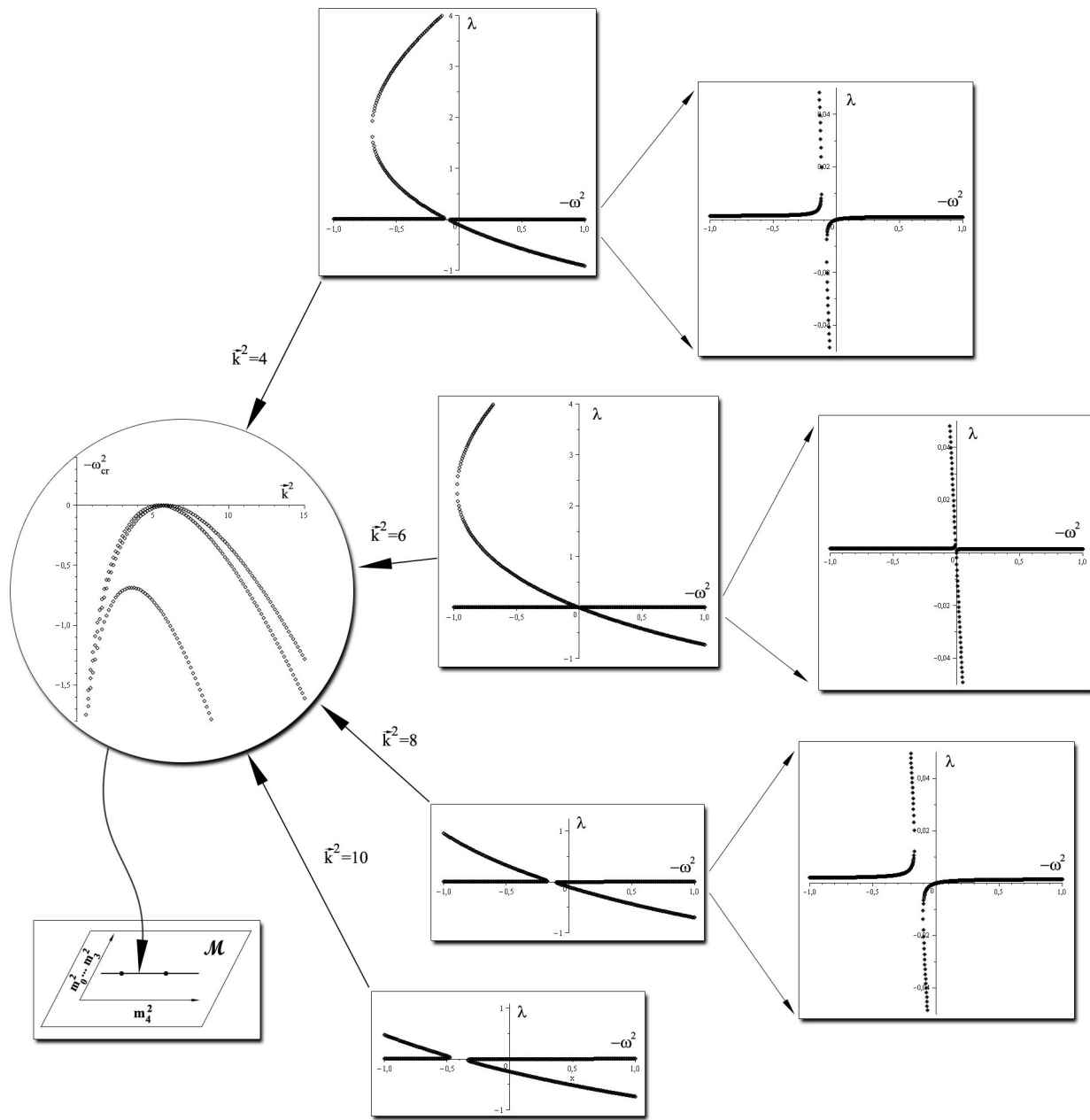


Figure 13: